Artūrs Suharevs

RESEARCH OF AIRCRAFT GROUND PATH CONTROL DEVICES AND OPTIMIZATION AT TAKEOFF AND LANDING STAGES

Summary of the Doctoral Thesis

RIGA TECHNICAL UNIVERSITY

Faculty of Mechanical Engineering, Transport and Aeronautics
Institute of Transport

Artūrs Suharevs

Doctoral Student of the Study Programme "Transport"

RESEARCH OF AIRCRAFT GROUND PATH CONTROL DEVICES AND OPTIMIZATION AT TAKEOFF AND LANDING STAGES

Summary of the Doctoral Thesis

Scientific Supervisor
Assoc. Professor Dr. sc. ing.
VLADIMIRS ŠESTAKOVS

RTU Press
Riga 2022

Suharevs A. Research of Aircraft Ground Path Control Devices and Optimization at Takeoff and Landing Stages. Summary of the Doctoral Thesis. – Riga: RTU Press, 2022. – 47 p.

Published in accordance with the decision of the Promotion Council "RTU P-22" of 18 January 2022, Minutes No. 04030-9.16/1.

DOCTORAL THESIS PROPOSED TO RIGA TECHNICAL UNIVERSITY FOR THE PROMOTION TO THE SCIENTIFIC DEGREE OF DOCTOR OF SCIENCE

To be granted the scientific degree of Doctor of Science (Ph. D.), the present Doctoral Thesis has been submitted for the defence at the open meeting of RTU Promotion Council on 20 May 2022 at 14.00 at the Faculty of Mechanical Engineering, Transport and Aeronautics of Riga Technical University, at 6B Ķīpsalas Street, Room 204.

OFFICIAL REVIEWERS

Professor Dr. sc. ing. Pāvels Gavrilovs
Riga Technical University

Professor Dr. habil. sc. ing. Krzysztof Szafran
Łukasiewicz Research Network – Institute of Aviation, Poland

Professor Dr. habil. sc. ing. Rafal Chatys
Kielce University of Technology, Poland

DECLARATION OF ACADEMIC INTEGRITY

I hereby declare that the Doctoral Thesis submitted for the review to Riga Technical University for the promotion to the scientific degree of Doctor of Science (Ph. D.) is my own. I confirm that this Doctoral Thesis had not been submitted to any other university for the promotion to a scientific degree.

Artūrs Suharevs ……………………………. (signature)
Date: ………………………

The Doctoral Thesis has been written in Latvian. It consists of an Introduction, 5 chapters, Conclusions, 87 figures, 11 tables, 1 appendix; the total number of pages is 99, including appendices. The Bibliography contains 49 titles.

TABLE OF CONTENTS

ABBREVIATIONS

AC or GK – aircraft

PNJ – runway

PNS – satellite navigation system

LEN – flight manual instruction

VJL – sea level

TRD – turbo reactive engine

TRB – inner radio marker beacon

ABS – anti-lock braking system

V_{mcg} – minimum ground handling speed

V_{mca} – minimum air speed (i.e. minimum liftoff speed)

V_1 – decision rate

V_R – rotation speed

V_{MU} – minimum adhesion rate at ground contact

V_{LOF} – liftoff speed

V_2 – safety liftoff speed

MKM – minimal square method

KGS – course glissade system

INS – inertial navigation system

ILS – instrumental landing system

FAR – federal aviation regulations

PSEU – proximity switch electronic unit

FMS – flight management system

GPS – global positioning system

GNSS – global navigation satellite system

INTRODUCTION

Subject actuality

Takeoff and landing are the starting and ending phases of the flight, which require maximum attention and precision from the pilots. Statistically they are the most dangerous phases of flight. In the takeoff process, the aircraft accelerates, pulls off the ground and takes the flight height assigned. The landing is conditioned by a slow movement of the aeroplane from the 15 m height to its full stop after landing and subsequent running down the runways. Landing is the most difficult flight phase, requiring high skills of pilots. The aeroplane landing process shall be initiated by maneuvers such as approaching the aerodrome and starting the landing. The landing consists of the following steps: height reduction, alignment, passage, landing and running. Aircraft takeoff is usually divided into two basic steps – takeoff and start height. These steps, in turn, include several other steps.

The progress of the aircraft industry in our days has reached the point that all these phases can be carried out without the pilot's involvement, i.e., through an automatic pilot system. In civil aviation, unmanned aerial systems are still in use, with a focus, a main leg in horizontal flight and crew control. However, the landing and takeoff process is being conducted with the help of experienced pilots. In view of the complexity and hazards of all activities to be carried out during the landing, the landing phase is, therefore, considered to be the statistically most hazardous. Figures 1.1 and 1.2 show the statistics on all incidents from 2009 to 2018 by categories. The statistics are taken from the slides of the Boeing Company presentation (Statistical Summary of Commercial Jet Airplane Accidents Worldwide Operations | 1959 – 2018 50th Edition
http://www.boeing.com/resources/boeingdotcom/company/about_bca/pdf/statsum.pdf)
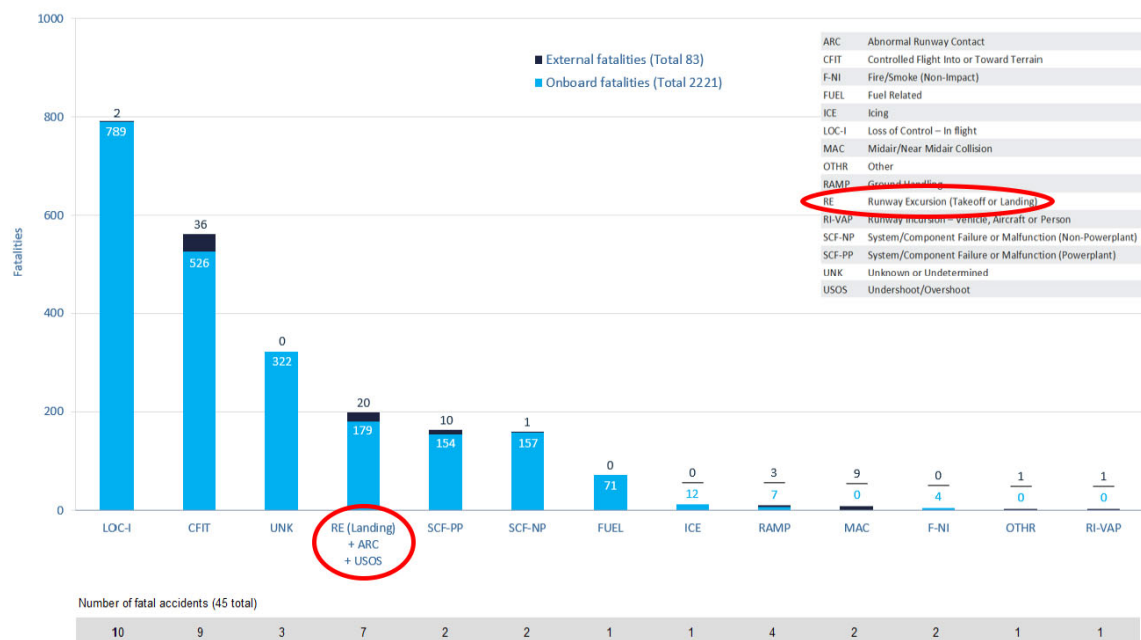
Fig. 1.1. Breakdown of the aircraft disaster for the period 2010–2019.

	Taxi, load/ unload, parked, tow	Takeoff (12%)	Initial climb	Climb (flaps up)	Cruise	Descent	Initial approach	Final approach	Landing (53%)
Fatal accidents	7%	4%	7%	13%	11%	2%	2%	29%	24%
Onboard fatalities	0%	5%	1%	20%	23%	3%	7%	30%	11%
		6%						41%	
Exposure (percentage of flight time estimated for a 1.5-hour flight)		1%	1%	14%	57%	Initial approach fix 11%	Final approach fix 12%	3%	1%

Note: Percentages may not sum to 100% because of numerical rounding.

Distribution of fatal accidents and onboard fatalities | 2010 through 2019
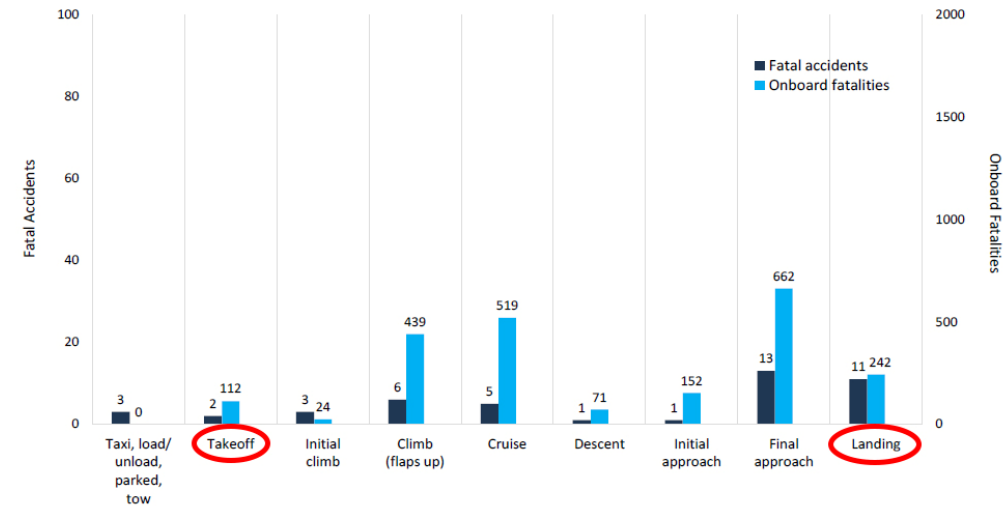

Fig. 1.2. Breakdown of accidents by flight.

It is obvious that the largest number of incidents and disasters are directly related to the takeoff and particularly landing phases.

It is quite difficult to focusing on this statistics because it is impossible to understand the nature of the disaster. In order to start tackling this problem, information was collected on a number of incidents, investigating the causes of incidents/disaster. Information was verified on how much of the incidents took place recently, as there is a possibility that all of these incidents occurred 10 years ago and are now out of date (the problem has been resolved). And the second problem is that not after all incidents the "investigation process" has been completed.

For those purposes, the http://avherald.com/ website was used, where nearly all incidents occurring worldwide are most common seen immediately after the event. Table 1.1 shows recent accidents involving the crossing of the runway border.

Table 1.1

Recent Accidents Related to the Border Crossing of Runway

Date	Status	AC reg.no.	Flight no.	Details from reports
04.07.2020	Incident	Boeing 747-400, LX-UCV	CV-7536	Hong Kong, rejected takeoff due to engine problem
14.06.2020	Incident	China Airlines A333, CI-202	B-18302	Taipei, all primary computers, reversers and autobrakes failed on touchdown, affecting the stopping distance of the aircraft. The crew applied maximum manual braking and managed to stop the aircraft 10 meters/33 feet ahead of the runway end (runway length 2600 meters/8530 feet).
01.07.2020	Incident	Garuda A333 PK-GHD	GA-613	Makassar, runway excursion during backtracking for departure.
14.06.2020	Incident	Vietjet A321	VJ-322	Ho Chi Minh City, runway excursion on landing.
03.06.2020	Accident	Fedex MD11 N583FE	FX-5033	landed on Mumbai's runway 14 at 12:14L (06:44Z) but overran the end of the runway by about 9 meters/30 feet.
22.05.2020	Incident	West Atlantic ATP SE-MAO	PT-425	Birmingham, temporary runway excursion on second approach.
06.01.2020	Incident	Thai Lion B739 HS-LTL	SL-180	Hanoi, runway incursion.
18.03.2020	Incident	Vietnam A321 VN-A392	VN-920	Ho Chi Minh City, rejected takeoff due to uncontained engine failure sets grass alight.
07.06.2020	Incident	Canada A320 C-FMSX	AC-329	Edmonton, autobrakes failure.
05.06.2020	Incident	Kalitta B734 N733CK	KI-822	Rochester, veered off runway on rejected takeoff.
05.06.2020	Incident	South Sudan Supreme AN26 S9-TLW	EK-26710	Renk, runway excursion at landing.
27.05.2020	Incident	Swift AT72 EC-INV	WT-6992	Cologne, rejected takeoff due to being aligned with runway edge lights.
27.06.2019	Accident	Angara AN24 RA-47366	2G-200	Nizhneangarsk, engine failure, veered off runway and collided with building.

An obvious problem remains very actual. Only in June 2020 there were at least six accidents (not all accidents are reflected in the portal).

Purpose of the Thesis

The purpose of the Thesis is to develop a system and methodology that could carry out, in an entirely automatic mode, the running and braking of the aircraft after landing on the runway in such a way as to make it maximally efficient and secure or at least to assist pilots in determining the length of the remaining braking and running road, respectively, until the end of the landing zone, taking into account the system output data from aircraft avionic equipment and taking into account other factors, such as weather conditions, brake and wheel conditions, various factor coefficients, acceleration/deceleration statistics, aerodynamic characteristics of the aircraft, etc. The Thesis also offers a technical solution (portable device) that will make it possible to change the landing/takeoff methodology in order to achieve the above target as well as to help with flight quality analysis and accident investigation for an aircraft that is poorly equipped with advanced flight and navigation equipment.

Tasks

In order to achieve this goal, a number of key tasks were set:

1) to assess the state of the problem and the causes of the incidents;

2) to investigate the current methodology (AC documentation and pilot/airline procedures) in the takeoff and landing phases;

3) to explore today's technical solutions and options to solve this problem with the equipment already in use (AC equipment and software provision; internal and outside);

4) to model and optimize the "system" of the aircraft track length in the takeoff and landing phases;

5) to develop a physical device (prototype) and an algorithm to:

• forecast and prevent accidents;

• efficiently and rationally use AC systems;

• facilitate the crew work;

• try to increase the flight safety;

• make it possible to analyze the quality of flights and to help with the investigation of flight accidents in light aircraft and aircraft that are poorly equipped with modern flight and navigation equipment;

6) to perform experiments and create the effectiveness of the idea.

An analysis of the aircraft braking and running track has been carried in the Thesis, and the need to develop an automated device capable of controlling the length of the aircraft's braking and running track after landing and takeoff is justified.

The device must be able to calculate the required parameters at every moment of time for rational use of the aircraft systems, to extend the deadline for the wear of the brakes, and to ensure the safety of the aircraft passengers and to allow for the exclusion of pilot errors.

Object of study – AC acceleration/braking methodology and technical capabilities.

Subject-matter – Any type of AC (Experimental/General/Civil aviation).

Place of study – any aerodrome.

The study uses the following scientific methods:

• mathematical modelling;

• algorithm modelling (Simulink);

• probability theory;

• processing of statistical data;

• performing an experiment.

Scientific novelty

Development and optimization of the AC braking/acceleration model.

A new methodology for the braking/acceleration phases of the AC due to the development of non-existing equipment (an algorithm based on data from the most accurate sensors equipped with almost all modern AC types).

Practical significance

• Reduction of incidents and accidents in landing/takeoff processes.

• Facilitating crew work.

• Increased flight safety.

• Extension of AC resources (status of components).

• Saving airline resources.

• Reduction of environmental pollution.

• Flight quality analysis and optimization.

Hypotheses to be defended

• The pattern of flight safety increase based on the new methodology and technical solution.

• Proof of the effectiveness and safety of a new acceleration/braking methodology.

• A technical solution for implementing a new methodology.

• Methodologies for economic and environmental efficiency.

Accuracy of the research results

All obtained research results are based on the author's practical calculations and trials.

Mathematical models, methods, algorithms, charts and ideas developed by the author have been tested in practice, and a new methodology has been put forward for takeoff/landing steps. The regulatory documentation does not permit the use/testing of the proposed method and equipment on commercial AC immediately – a number of further steps are needed to certify a method and technological solution with the involving of Part-21 organization and a special permit from the AC type manufacturer.

Approbation of the research

The research results were presented at two international scientific conferences in Lithuania and Latvia, seven publications included in three scientific journals.

Participation in international scientific conferences

1. Kaunas University of Technology, 24th International Scientific Conference TRANSPORT MEANS 2020, PALANGA, 30 September – 2 October 2020; Report: "Safety Management System development for airline"

2. The 5th International Scientific and Practical Conference TRANSPORT. EDUCATION. LOGISTICS AND ENGINEERING – 2018
   "DEVELOPMENT OF METHODOLOGY FOR SAFETY RISK – BASED AIRLINE" A. Bitins, L. Mikelson, A. Suharevs.
   "АНАЛИЗ ФАКТОРОВ ВЛИЯЮЩИХ НА ДЛИНУ ПРОБЕГА САМОЛЕТА ПО ВПП" A. Suharevs

3. Riga Technical University 56th Scientific International Conference, Riga (Latvia) 20.05.2015, "Gaisa kuǵa borta kontroles ierīču pētniecība un optimizācija pacelšanas un nosēšanas etapos", A. Suharevs.

4. Riga Technical University 57th Scientific International Conference, Riga (Latvia) 17.10.2016, "Gaisakuǵa pacelšanās un nolaišanās zemes ceļa garuma skaitļošanas sistēma", A. Suharevs.

5. Riga Technical University 60th Scientific International Conference, Riga (Latvia) 16.10.2019, "Mikrokontrolieru izmantošana aviācijas nozarē", A. Suharevs.

6. Riga Technical University, 12.11.2015, Zinatniskais seminars," Gaisa kuǵa borta kontroles ierīču pētniecība un optimizācija pacelšanās un nosēšanās etapos".

7. Riga Technical University, 09.02.2017, Zinātniskais seminārs, "Pacelšanās-nolaišanās skrejceļa skaitīšanas ierīces strukturāla shēma"

Publications

1. Arthur Suharev, Vladimir Shestakov, Leonid Vinogradov. "Estimation of evacuation time of passengers in aircraft accidents with fire in airfield areas". AVIATION ISSN: 1648-7788 / eISSN: 1822–4180. Article in Press. https://doi.org/10.3846/aviation.2020.12653

2. Arthur Suharev, Vladimir Shestakov, and Konrad Stefanski. "Analysis of the affecting factors on aircraft takeoff and landing ground path length". AIP Conference Proceedings 2077, 020056 (2019); https://doi.org/10.1063/1.5091917. Published Online: 21 February 2019

3. A. Bitins, L. Mikelson, A. Suharevs. "Development of methodology for safety risk – based airline". The 5th International Scientific and Practical Conference. Transport. Education. Logistics And Engineering – 2018. Proceedings. ISBN 978-9984-9996-8-5

4. A. Suharevs. "Анализ факторов влияющих на длину пробега самолета по ВПП". The 5th International Scientific and Practical Conference. Transport. Education. Logistics And Engineering – 2018. Proceedings. ISBN 978-9984-9996-8-5

5. Artūrs Suharevs, Pjotrs Trifonovs-Bogdanovs, Vladimirs Šestakovs, Konstantin Mamay. "Dynamic Model of Aircraft Landing". Riga Technical University. Transport and Aerospace Engineering. ISSN 2255-9876 (online). ISSN 2255-968X (print). December 2016, vol. 3, pp. 38–43. doi: 10.1515/tae-2016-0005. https://www.degruyter.com/view/j/tae

6. A. Suharevs. "Gaisakuǵa zemes ceļa garuma skaitļošanas sistēma pacelšanās un nolaišanās brīdī". The 4th International Scientific and Practical Conference. Transport Systems, Logistics And Engineering – 2016. Proceedings. ISBN 978-9984-9996-6-1

7. Arthur Suharev, Jevgenij Tereshchenko, Vladimir Shestakov, Zarif Zabirov. "Identification of abnormal situations in flight". AVIATION (In Press).

1. TAKEOFF AND LANDING DYNAMICS AND KINETICS

1.1. Run path length

The length of the run is called the road by which the aircraft takes place from the start to the point of withdrawal from the ground. The length of the run is one of the main values for the characteristics of the aircraft, by which the required takeoff/landing runway length is determined.

The takeoff distance (S, $TOFL$) consists of a running distance (S_g, S_{TOG} – ground run) during which the speed (V_{LOF}) and takeoff in the first air segment (S_a, S_{TOA} – airborne distance) are reached, during which the safe climb rate (V_2) and the minimum height prescribed in the regulatory documents are reached (normally) $h = 11$ m (35 ft) – CS-25 (Certification Specifications for Large Aeroplanes) or 15 m – CS-23, depending on the aircraft type).
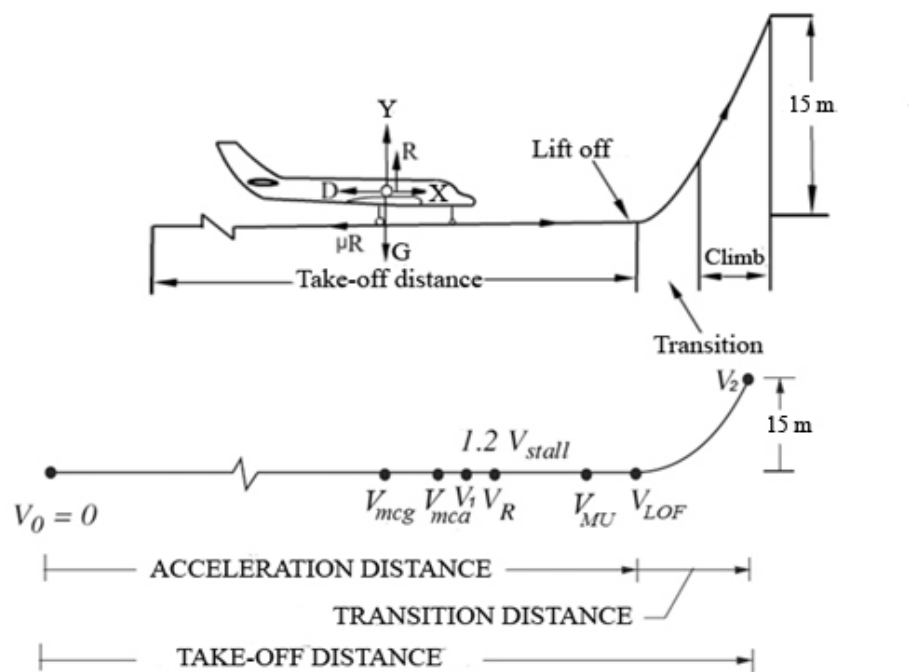

Fig. 1.5. Important takeoff moments and lengths.

Figure 1.5 shows the following speed parameters at takeoff:

V_{mcg} – minimum ground handling rate;

V_{mca} – minimum air handling rate (so-called breaking speed when detaching from the ground);

V_1 – decision rate (critical engine load rate);

V_R – lift speed L ≥ W (allowing safe lifting of front-end wheels from the surface);

V_{MU} – minimum adhesion rate, at ground contact;

V_{LOF} – minimum lift rate;

V_2 – takeoff elevation security speed.

12

The most important of these are the decision-making speed – V_1 (whether to continue or stop taking off), the pull-off speed – V_{LOF} or V_{atr} (possible to pull away safely from the runway) and the takeoff speed – V_2 (it is possible to safely continue the initial climb).

When viewing the aeroplane's run as an evenly accelerated movement with acceleration t_{vid}, it can be concluded (at no wind) that the average run time will be:

$$t_{vid} = \frac{v_{atr}}{i_{vid}} \; , \tag{1.1}$$

where average speed is:

$$v_{vid} = \frac{v_{atr}}{2} \; , \tag{1.2}$$

but as a run length

$$L_{ieskr} = v_{vid} * t \; , \tag{1.3}$$

as a result:

$$L_{ieskr} = \frac{v_{atr}^2}{2i_{vid}} \; . \tag{1.4}$$

As follows from the formula (1.12), the length of the run depends mainly on the speed of pulling back and the average acceleration during the run.

For an estimated assessment, the following formula may be used for the effects of individual parameters:

$$L_{ieskr} = \frac{v_{atr}^2}{2g\left(\dfrac{P_{vid}}{G} - f\right)} \; , \tag{1.5}$$

where P_{vid} is aircraft thrust capacity; and f is the friction coefficient.

1.2. Braking path length

Braking path length L_{nosk} is the distance taken by the plane after touching the ground to the moment until it stops completely. The calculation of the length of the run-off is analogous to the calculation of the length of the takeoff roll, only by the difference that the acceleration at landing is negative. As well as at the lifting roll, an average acceleration value may be used for an estimate of the length of the run, when the movement is viewed as uniformly slow with an end speed equal to zero and at the starting speed in V_{nos}. Taking into account the effects of the wind, the formula for determining the length of the run-off path is as follows [46, *308*]:

$$L_{nosk} = \frac{\left(V_{nos} \pm W\right)^2}{2j_{vid}} \; , \tag{1.6}$$

where j_{vid} is average plane braking acceleration module; $\pm W$ is longitudinal wind speed component ("+" is used at the wind of the road, but "–" is the sign at the counter-wind).

The formula for determining the average braking acceleration with the impact of the tilt is obtained as follows [46, *308*]:

$$j_{vid} = -\frac{\left(X_a + F_{br} \pm mg\sin\theta\right)_{vid}}{m} \ , \tag{1.7}$$

where

j_{vid} – average braking acceleration at run-off;

m – landing mass of the airplane;

$mg\sin\theta$ – longitudinal plane weight component ("+" mark is applied at takeoff to an angle, "–" – under the angle);

F_{br} – aircraft friction force;

vid – average value throughout the braking length;

X_a – aerodynamic resistance force.

From the Formulae (1.6) and (1.7), it is apparent that the length of the run is influenced by those factors that affect the lowering speed and the average braking acceleration.

1.3. Description of the dynamic pattern of the aircraft

Designing the plane's movement model in landing mode is pretty challenging. This is due to the fact that the movement of objects is different during landing. In the initial landing phase, when the object approaches the runway, there are aerodynamic forces and moments that work on it, as well as gravity. In this situation, the object is an airplane with its own laws of movement. But as soon as the wheels of the object touch the runway, a new force works on the object, and other forces differ. The friction force is starting to work on the object, the aerodynamic forces are starting to shrink. The friction force of the wheels depends on the size of the aerodynamic hoist (relative to the weight of the object). The more time the object moves around the runway, the less aerodynamic elevation and the greater is the strength of wheel friction. The plane, in its kinematic behavior, transforms itself into a road transport car.

The plane's longitudinal movements in the aircraft phase are described in equations according to(1.8):

$$m\frac{dV_x}{d\bar{t}} + m\left(\omega_y V_z - \omega_z V_y\right) = \sum F_x \ ,$$

$$m\frac{dV_y}{d\bar{t}} + m(\omega_z V_x - \omega_x V_z) = \sum F_y \ , \tag{1.8}$$

$$I_Z\frac{d\omega_Z}{dt} = \sum_{i=1}^{m} M_{Z_i}$$

where on the right side of the equations are aerodynamic forces and moments that act on the plane.

The forces operating on the plane during flight and the plane's movement parameters in the vertical plane are shown in Fig. 1.13.
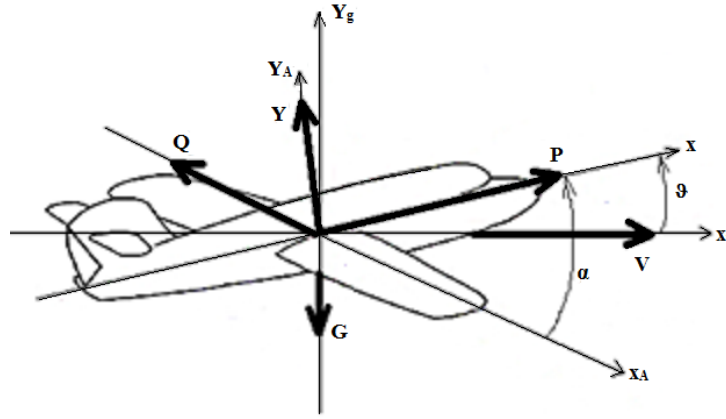
Fig. 1.13. Forces operating on an airplane during its horizontal flight.

Aerodynamic forces, such as lifting Y and towing X, act on the aircraft during flight:

$$Y = C_y S \frac{\rho V^2}{2}, \tag{1.9}$$

$$X = C_x S \frac{\rho V^2}{2}$$

where

C_y, C_x – aerodynamic friction coefficients;

S – wing area;

ρ – air density;

V – wind speed.

Gravity force G and aircraft engine power P operate on the aircraft during its flight.

The equation describing the linear movement of the aircraft shall then be written as follows:

$$m \left(\frac{dV_x}{dt} + \omega_y V_z - \omega_z V_y \right) = P_x - X - G \sin \theta, \tag{1.10}$$

$$m \left(\frac{dV_y}{dt} + \omega_z V_x - \omega_x V_z \right) = Y - G \cos \theta.$$

Adding kinematic equation:

$$V_y = \frac{dH}{dt} = V_0 \sin \theta, \tag{1.11}$$

$$V_x = \frac{dL}{dt} = V_0 \cos \theta ,$$

where V_x, V_y are the components of relative speed along the axes of the ground coordinate system.

The dynamics of the site in the ground transport phase will change significantly compared to the movement of the object in the aircraft phase described in Equations (1.10 and 1.11), as the object's movement on the runway surface will impose certain limits on the film and dynamics of the site.

The object's movement on the runway surface will cause many changes to the object's kinematic parameters. The object's angular speed will not be ($\omega x = 0$; $\omega y = 0$; $\omega z = 0$) because there will be no angular movement of the object. The slope angle of the trajectory θ will be equal to zero. The flow angles α and pitch ϑ will be constant and equal to ($\alpha = \vartheta$).

The forces acting on the object during its movement along the runway will also change compared to the force operating on the flight (Fig. 1.13). The purpose of this flight phase is to reduce the flight speed of the plane. So, there will be no jet engine traction (P). The force will be created by operating the plane in the opposite direction at a speed.

15

After the aircraft's wheels touch the runway, the thrust direction P of the aircraft's engine is inverted compared to the flight phase. The crew must do this with a special reversing device at the initial stage of the movement along the runway at a very high speed. Reducing the speed of the aircraft wheels by braking the wheels causes intense tire wear. Therefore, this braking method is not applicable in the first phase of aircraft movement on the runway. The reversing (reverse) device shall only be used during a relatively small period of operation along the runway in order to reduce the plane's speed intensively enough at the initial stage of its motion along the runway. Therefore, during the braking process, the engine thrust of the aircraft will only operate in a negative direction within a specified time interval (–P(Δt)).

Aerodynamic forces operating on the plane during flight will also affect the plane's movement on the runway. The towing force **X** will continue to operate counter to the speed of the aircraft that acts on it with the braking effect (reducing its speed). The size of the towing **X** will be reduced over time as it will reduce the speed of the aircraft (1.9). Another force of aerodynamic resistance will be created on the plane's movement – a force of spoiler resistance **X_sp**. The **X_sp** force of the spoiler resistance is created by special wing flaps that are prone to flow.
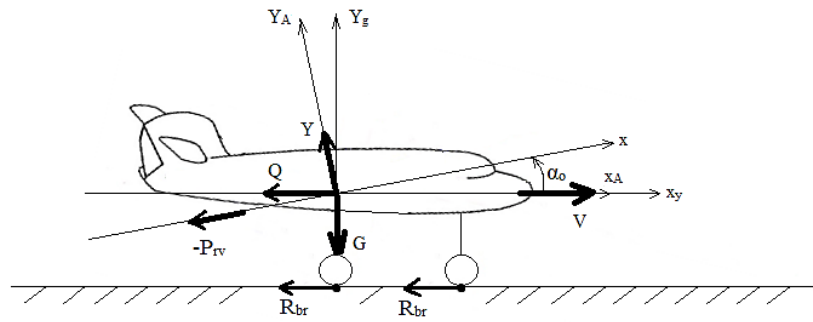

Fig. 1.14. Forces operating on the plane during landing.

There is a new braking force typical of the plane's movement along the runway. This is the wheel shaft rotation braking force F_{fr}. This force consists of 2 components. The first component F_{fr1} stems from the force interaction between runway surfaces and aircraft wheels. It is the force of rolling resistance. The size of the rolling resistance force shall be determined (in literature) as:

$$F_{fr_1} = k_{fr_1} G, \qquad (1.12)$$

where k_{fr_1} is the rolling resistance factor, and G is the AC weight.

The rolling resistance factor k_{fr1} (1.13) depends on the aircraft speed V (mph) and the runway position factor C_{st} (humidity, icing, etc.):

$$k_{fr_1} = (0.0041 + 0.000041V)C_{st} . \qquad (1.13)$$

The runway condition factor C_{st} can vary greatly. In particular, the dry flat concrete C_{st} will be 1.0.

The rolling resistance force F_{fr1} (1.12) in the case of the aircraft braking process is:

$$F_{fr_1} = k_{fr_1}(G - Y), \qquad (1.14)$$

where Y is the lifting value.

The lifting rate Y decreases over time (1.9) as the object's braking reduces its speed (V). The weight of the object (G) will remain the same as at the last moment of the flight (when the wheels of the object touch the runway). That is, the amount of rolling resistance force F_{fr1} is

minimal when aircraft wheels touch a point on the runway. When the aircraft moves on the runway, the rolling resistance force F_{fr1} will occasionally increase.

The second component of the rolling resistance force $F_{fr2}(pd)$ occurs when the object wheel shaft rotation braking device is carried out by the pilot by pressing the brake pedal. It is the engine of the plane's movement braking process. By intuitively creating the value of the wheel braking force, the pilot decreases the plane's speed to predetermined values during the period when the aircraft moves on the runway, thereby avoiding the aircraft running over the runway. In this process, it is also important (especially for civil aviation) to make an optimal choice of wheel braking force value so that tire wear is the least possible.

In order to implement the optimum braking process, the pilot should foresee the effect of the braking force on the cinematography of the aircraft. It is a very difficult task. A special device that, after each pilot rupture operation, will show the length of the following run after the creation of a special braking force, can help to solve this problem qualitatively.

In order to optimize the structure and assess the errors of the instrument with regard to the selection of different design parameters, the work of the specialized forecasting tool should be analyzed. This can be done on the dynamic model of the plane landing.

Landing dynamics and kinetics analysis allow you to perform the plane landing pattern. From Equations (1.10 and 1.11), we get the dynamic plane landing pattern:

$$m\frac{dV}{dt} = -P(\Delta t) - X - F_{fr_1} - F_{fr_2}(pd) - K_{1_{U_x}}U_x - K_{2_{U_y}}U_x, \qquad (1.15)$$

$$L_{xz}(t) = Vt$$

where $L_{xz}(t)$ is the landing distance of the aircraft on the runway and $K_{1Ux}\,U_x$, $K_{2Uy}\,U_x$ are wind disturbances from the horizontal wind speed component U_x.

In the dynamic pattern of the airplane, all forces must be placed in a specified way, depending on the conditions of the landing. The reverse force P of the engine of the aircraft must be taken from the specific parameters of the aircraft's engine landing mode. Aerodynamic forces such as lifting Y and towing X are very easy to calculate because the values of these forces depend only on the plane's speed (1.9). It is necessary to enter the Cy and the Cx factor dependency on the aircraft speed in the aerodynamic forces and to apply the aircraft speed in their input. This will create feedback on the model. For the calculation of the rolling resistance force F_{fr1}, the weight of the aircraft must be continuously reduced by the lifting force.

Wind disturbance $K_{1Ux}U_x$, $K_{2Uy}U_x$ from the horizontal wind speed component U_x will be determined from an aerodynamic force expression (1.9). In the case of U_x, the size of the aerodynamic forces X and Y also changes and becomes interference factors in the movement of the aircraft. The magnitude of the interfering factors is determined as the expansion of the X and Y components of the aerodynamic forces according to the U_x parameter:

$$K_{1_{U_x}}U_x = \Delta X = \left(C_x^V S \frac{\rho V^2}{2}\right)U_x + \left(C_x S \frac{\rho 2V}{2}\right)U_x = \frac{S\rho V^2}{2}\left(\frac{C_x^M}{a_H} + \frac{2C_x}{V}\right)U_x, \qquad (1.16)$$

$$K_{2_{U_y}}U_x = \Delta Y = \left(C_y^V S \frac{\rho V^2}{2}\right)U_x + \left(C_y S \frac{\rho 2V}{2}\right)U_x = \frac{S\rho V^2}{2}\left(\frac{C_y^M}{a_H} + \frac{2C_y}{V}\right)U_x$$

Factors $K_{1Ux,}\,K_{2Uy}$ in the dynamic pattern of the aircraft landing are then defined as:

$$K_{1_{U_x}} = \frac{S\rho V^2}{2}\left(\frac{C_x^M}{a_H} + \frac{2C_x}{V}\right)U_x, \qquad (1.17)$$

$$K_{2_{U_y}} = \frac{S\rho V^2}{2}\left(\frac{C_y^M}{a_H} + \frac{2C_y}{V}\right).$$

The aircraft control braking force $F_{fr2(pd)}$ (1.15), resulting from the rotation braking process of the aircraft wheel shaft when the pilot is pressing the brake pedals, must be modelled by applying at different times the constant signals corresponding to the model pilot's strength. These values, $F_{fr2(pd)}$, can be entered into the experiment participant model by rendering the trial operation at the landing stage.

1.4. The plane's movement on the runway during landings. Mathematical model

A previous subsection described components of the dynamic model of the plane's landing. Each component was discussed and its role in the landing process was explained. The author also provides appropriate formulas that describe each component of the next model. For mathematical models, however, some of these formulas are complex or poorly adapted to be used in modeling. Therefore, the formulas and equations from the previous subsection are better transformed into a form that will be convenient for modeling and analysis.

From Equations (1.10 and 1.11), we obtained the dynamic plane landing pattern (1.15), but these equations are written in general form and should be described in detail.

Let us convert the first part of the dynamic model (1.15) into the following form:

$$m\frac{dV_x}{dt} = -P_x - X - F_{fr_1} - F_{fr_2}(pd) ,\tag{1.18}$$

where

$-P_x = P\cos\alpha_0;$
X – resistance component (1.9);
F_{fr1} – rolling resistance force (1.14);
Y – lifting force (1.9);
F_{fr2} (pd) – resistance component at the time the pilot is pressing on the brakes.

The airplane air speed V, used in aerodynamic force formula consists of two components – the lifting component Y and the towing component X (1.9):

$$V = V_{airplane} \pm U ,\tag{1.19}$$

where $V_{airplane}$ is AC speed and U is wind speed.

The V_x component in Equation (1.18) is the plane's ground speed (the speed relative to the ground). In our case, V_x should be treated as the speed of the plane relative to the runway. It will, therefore, be written as follows:

$$V_x = V_r\tag{1.20}$$

The value of "m" in Equation (1.18) is equal to:

$$m = \frac{G}{q} ,\tag{1.21}$$

where G is AC weight and $q = 9.81$ m/s^2 is acceleration of gravity.

After all these transformations, we are prepared to write Equations (1.15) in the form of the following equations system:

$$\begin{cases} \frac{dV_r(t)}{dt} = -\left(\frac{q}{G}\right)P_x(\Delta t) - \left(\frac{q}{G}\right)\frac{C_x S\rho}{2}\left(V_{airplane} \pm U\right)^2 - \frac{k_{fr_1}q}{G}\left(G - \frac{C_y S\rho}{2}V^2\right) - F_{fr_2}(pd) \\ L(t) = \int_0^t \left(V_{r_0} - \Delta V_r\right) dt , \end{cases}\tag{1.22}$$

where V_{ro} is the touchdown speed (at the touching point of the runway); $P_x(\Delta t)$ is engine reverse during time Δt; and L(t) is AC landing rolling distance.

Let us now transform the equation system (1.22) into a form that is useful for further modelling and analysis :

$$\begin{cases} \dfrac{dV_r}{dt} = -K_G \left[P_x(\Delta t_{pc_i}) - K_x C_x V_a{}^2 - k_{fr_1}\left[G - K_y C_y V_a{}^2 \right] - F_{fr_2}(pd) \right] \\ L_r(t) = \int_0^t \left(V_{r_0} - \Delta V_r \right) dt \end{cases}, \qquad (1.23)$$

where

$$K_G = \frac{q}{G};$$

$$\Delta t_{pc_i} = \Delta t_{r_0} + t_2 = const; K_x = K_y = \frac{S\rho}{2};$$

$$V_a = V_r \pm U.$$

This transformation is done by combining some elements of the system of the original Equation (1.22) and treating them as one factor. Most of these elements of the equations system are unchanged and depend solely on the type of the plane tested and its parameters (weight, wing area typical of these aerodynamic force factors, etc.). It is, therefore, easier to combine them for further analysis and investigation, and thus to simplify the mathematical model for the development of equipment.

Finally, the initial equation system (1.22) will be transformed into the next equation:

$$\begin{cases} a_r = \dfrac{dV_r}{dt} = -K_G \left[P_x\left(\Delta t_{pc_i}\right) - K_x C_x V_a{}^2 - k_{fr_1}\left[G - K_y C_y V_a{}^2 \right] - F_{fr_2}(pd) \right] \\ L(t) = \int_0^t V_r\, dt \\ V_r = V_{r_0} - \Delta V_r \\ V_a = V_r \pm U \end{cases} \qquad (1.24)$$

where

$\Delta t_{pc_i} = \Delta t_{r_0} + t_2$; t_{ro} – reverse system activization time relevant to touchdown point;

t_2 – actual time of reverse mode.;

$F_{fr2}(pd)$ in Equation system (1.24) are the wheels of the chassis the braking force of which is actuated by the pilot.

Equation system (1.24) is a dynamic model for the plane's movement along the runway, where the length of the plane's landing is determined.

The functional modeling task of the aircraft's runway landing control (which performs the functions of the forecasting device) is more extensive than simply determining the length of the runway landing. The mathematical model of the plane's runway movement is only part of the modeling task of the plane's runway landing control.

The main task of modelling the work of the aircraft runway landing control is the distinction between the original runway length L_r (residual runway length from the airplane landing point to the end of the runway) and the determination of the runway running length ΔL_r (Fig.1.16).
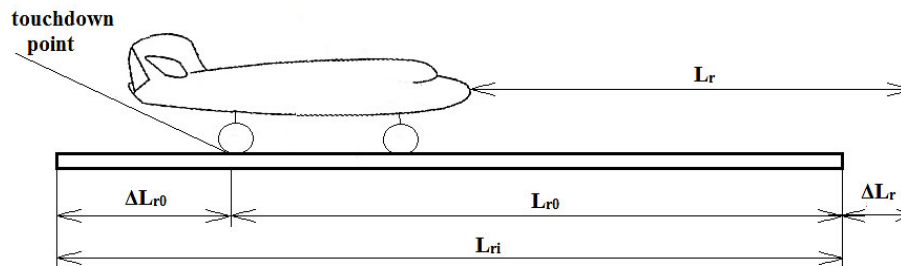
$$\Delta L_r = L_{r0} - L_r \qquad (1.25)$$

Fig. 1.16. Runway distances used in the plane's runway landing control.

19

To solve the problem of the plane's runway landing control work model, the geometrical equations of the plane's movement must be added to the equations of the plane's pattern of movement :

$$L_{r_0} = L_{r_i} - \Delta L_{r_0}$$
$$\Delta L_r = L_{r_0} - L_r \tag{1.26}$$

where

ΔL_r – runway remaining length;

L_{ri} – runway length;

ΔL_{r0} – "lost" length of runway this landing time;

L_{r0} – "real" runway length of this landing time.

Finally, we can get a full mathematical model for the work of the plane's runway landing control model by combining Equation systems (1.24) and (1.26):

$$\begin{cases} \dfrac{dV_r}{dt} = a_r = -K_{}P_x\left(\Delta t_{pc_i}\right) - -K_Q C_x(V_a)V^2 - K_K\left[G - K_y C_y(V_a)V^2\right] - F_{fr_2}(pd) \\[2mm] L(t) = \int_0^t V_r\, dt \\ V_r = V_{r_0} - \Delta V_r \\ V_a = V_r \pm U \\ L_{r_0} = L_{r_i} - \Delta L_{r_0} \\ \Delta L_r = L_{r_0} - L_r \end{cases} \tag{1.27}$$

In the device output, we can get two possible results:

- if the estimated runway spare length ΔL_r is positive (+ ΔL_r), the landing will be successful and meet all the requirements (the landing is satisfactory);

- if the estimated runway spare length ΔL_r is negative ($-\Delta L_r$), the plane landing does not fall within the runway and the landing is considered unsatisfactory.

Development of a dynamics model flowchart

In so far, as all the necessary theoretical information on the dynamics model of an aeroplane during the landing procedure is available, all factors are described and calculated, it is possible to start developing the diagram of the dynamics model block and verifying its operational validity.

To develop a dynamics pattern flowchart, we need to use the dynamics model Equation system (1.24). In this case, a complete and definitive system of Equations (1.27) is not necessarily required, since we are now developing only a dynamics model and a system of Equations (1.24) that will be sufficient to meet this task.

It is decided to use the MathWork MATLAB and SIMULINK software to create and verify the correct functioning of the landing dynamics model. The choice is based on a number of reasons, such as good application functionality, availability of necessary components to create a dynamics model, use of the machine, ease in changing components if something goes wrong, etc.

According to Equation (1.24), there are several input components that the user has set at the beginning of the simulation procedure, depending on the objectives of the observation: engine reverse traction mode P_x, landing rate V_r, rolling resistance force F_{fr2}, wind value U, and plane weight G. These input components can be easily changed, for example, if other planes are selected. There are also a number of constant and variable factors that were discussed and described above. Finally, the following flowchart was obtained (Fig .1 .21):
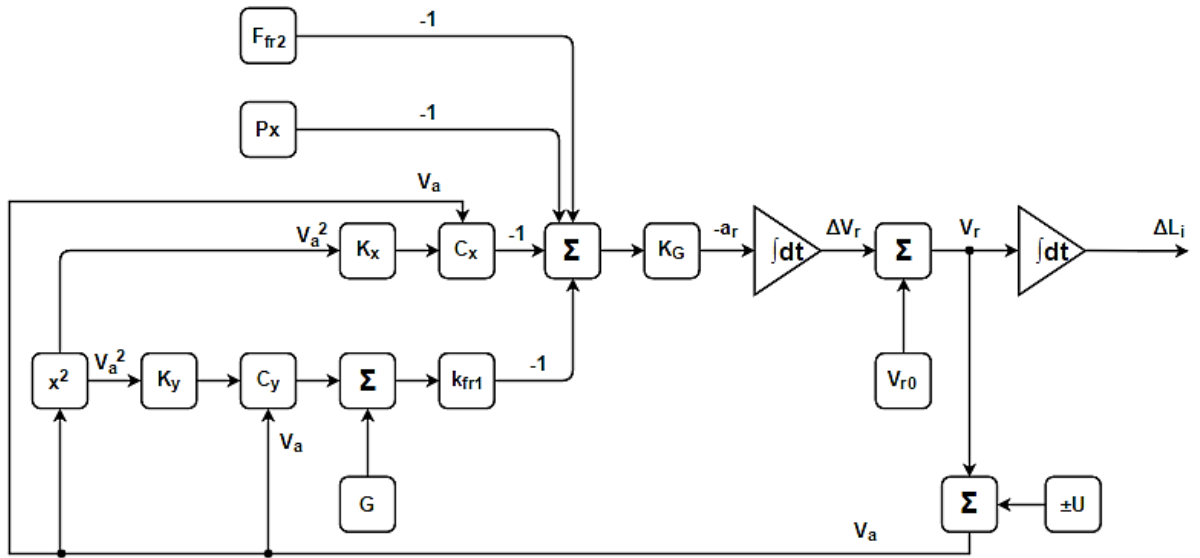
Fig. 1.21. Dynamics model flowchart.

As we see, this flowchart contains all the components described in Equation (1.24). The dynamics model block scheme can be divided into several channels, which ensure the correct functioning of the model as a complete system, but can also operate separately depending on what is to be analyzed. The first channel is brake force F_{fr2} generated by the movement of the brake pedals. It goes to the summing device, then to amplifier K_G, then, it is followed by the first integrator, summing up a device in which it is aggregated with landing rate V_{r0}, and finally, through the second integrator after which the required length of the landing run is obtained. As you see, it is one of the simplest channels in the flowchart because it does not have any feeds or crossings with other channels.

The second channel is an engine reverse traction circuit that is identical to the brake pedal circuit. It has the same path and elements and is very simple, without feeding or crossing with other channels.

The third channel of the dynamics model is the chain of the pull force. This channel is more complex because it has no direct input that is different from the two channels described above. Two feeds are taken after the incoming signal is summed at the required landing speed. The first feedback signal is variable factor C_x, which depends on the speed value and all the time a new speed is reached. The second feedback signal is inverted and reported with a coefficient K_x. The speed of the plane changes as the force is changing.

The last channel is the most sophisticated. It is the braking force caused by the braking force of the wheel movement. There are two feeds, as in the case of a towing force channel, but there is also a summing device in which the lifting force generated during this time interval is summed up by the weight of the plane. The lifting force is negative and the weight is positive. The smallest value after the summing device will be at the connecting point when these two components are practically the same, but then the weight of the plane will reduce the lifting force.

2. PROBLEM ANALYSES

Since at least half of the various aviation accidents occur in the takeoff and landing phases, the regulatory documents strongly define requirements for both aerodromes and aircraft parameters that can be operated safely under the appropriate conditions.

These days no aircraft is equipped with a system capable of calculating and predicting the plane's running and braking path against the end of the runway. Quite often it leads to tragic consequences. According to the Boeing's statistics (Fig. 1.1), the landing and takeoff phases are the most dangerous of all flight phases and represent 47% of all accidents, although the takeoff and landing processes takes only a few percent of the entire flight time. By providing the system for aircraft, it will be possible to reduce the number of accidents especially during landing, when the braking force is usually selected at a maximum under normal conditions, leading to a relatively high level of wear and brake wear. On the other hand, overly passive braking by the crew can lead to tragic events or, at best, to an incident (runway excursion). If the aircraft had at its disposal a device that could detect a potential accident (the absence of a runway length for braking and running), many accidents could be prevented (timely increasing the braking force, takeoff aborting, going to the second landing circle, etc.). The success of these phases depends heavily on the human factor, pilots experience, the technical condition of the aircraft and the weather conditions.

These factors can be recorded in the form of functional dependency. The determining factor is the actual running distance (L_{nosk}) by which the possibility of an aircraft runway excursion can be established as a the following function:

$$F\left(L_{nosk}\right) = \left\{ \begin{array}{c} f_1\left(x_1, x_2, \ldots, x_n\right), f_2\left(y_1, y_2, \ldots, y_m\right), f_3\left(z_1, z_2, \ldots, z_k\right), \\ f_4\left(q_1, q_2, \ldots, q_s\right), f_5\left(k_1, k_2, \ldots, k_t\right) \end{array} \right\} \quad (2.1)$$

where: f_1 – a function that depends on meteorological conditions;

$(x_1, \ldots, x_n)$ – runway condition (dry, wet, covered with water, muddy, etc.); actual landing wind and other factors;

f_2 – the function of the lifting-dragging changes performance of the airplane;

$(y_1, \ldots, y_m)$ – plane configuration (flaps/slats, aileron, spoiler position);

f_3 - the function of the piloting technique;

$(z_1, \ldots, z_k)$ – takeoff method; landing speed; height at the beginning of the runway; airplane passage time above the runway; engine force indicators, starting position of braking or running on the runway, etc.;

f_4 – function of the technical condition of the airplane;

$(q_1, \ldots, q_s)$ – engine condition; brake condition; anti-slip system condition; reverse condition for the engines; ground spoiler condition, etc.;

f_5 - a function that depends on the runway construction and location;

$(k_1, \ldots, k_t)$ – negative drop, positive elevation, variable wave drop; aerodrome height (reduced atmospheric pressure increases flight speed), etc.

2.1. Runway

Runway is the part of the aerodrome that is developed for takeoff and landing phases. Runway shall be specially prepared and equipped with a ground surface band with artificial or simple ground covering designed to ensure possibilities of aircraft to take off and land.

Runway length

Not all airports have great runway length, which also is the main reason for the problems relating to the plane's excursion from the runway.
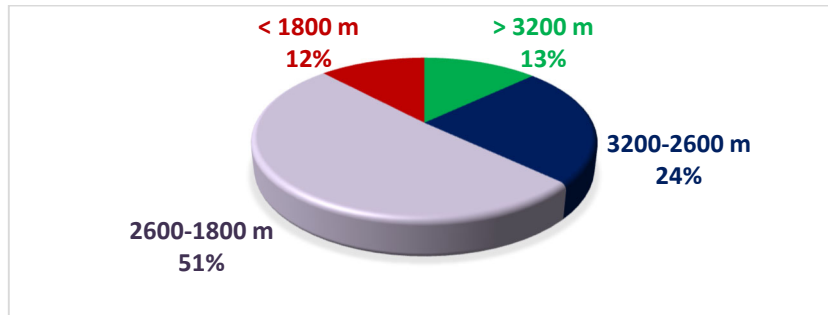

Fig. 2.1. Risk-sharing chart of the runway excursion possibility.

As shown in Fig. 2.1, 63 % of aerodromes may be associated with an increased level of runway excursion risk at takeoff and landing.

Depending on the length of the runway, the safety distances and the width on which airplanes with a defined wing swing and the base of the main chassis are capable to operate, there are 5 class aerodromes.

For any airfield class, the aircraft must provide both continued and interrupted flights, both on dry and wet runways.

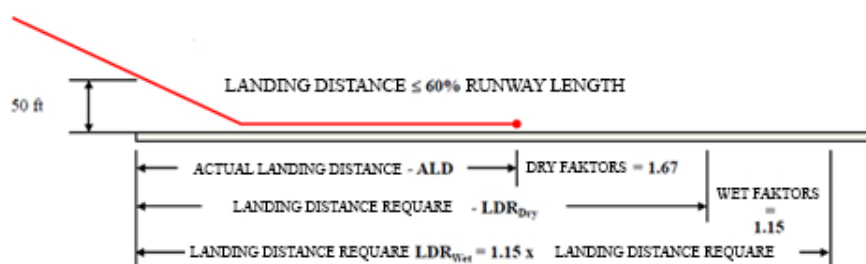Required length of dry and wet runway:

Fig. 2.2. Required runway length in according to **CS-25** *(Certification Specifications for Large Aeroplanes).*

Runway marking

The runway markings are needed, firstly, for a more accurate and secure landing of the aircraft on it. Runway markings are very different from those we are usually accustomed to seeing on car roads.

Fig. 2.3. Runway markings.

In Fig. 2.3 from left to right:

- **Safety bar GDJ** (yellow needle strips). Designed to protect the surface of the ground from exposure to powerful jet engines (so as not to damage the surface, not to raise dust, etc.) as well as for the reason not to excurse from runway. Airplanes are forbidden from being in the GDJ zone because its surface is not designed for their weight.
- **Displaced threshold** or displaced start (white arrows). Runway area where steering, running and running is allowed, but not landing.
- **The threshold** or stop (white bands in the form of "zebra") – the beginning of the runway, indicates the place where landing can be started. The threshold is designed to be spotted from afar. The number of lines depends on the width of the runway.
- **Marking number** and, if necessary, a letter (L – left, R – right, C – central).
- **Landing area:** double, parallel rectangles starting 300 m from the runway threshold.
- **Fixed distance marks** (large rectangles spaced every 150 m). When performing an ideal landing, the pilot with his eyes "holds" the landing area, and the touchdown takes place on the grounding area.

The legend attributes are also the center line and, in some cases, the side lines are required.

3. AIRCRAFT BRAKING POSSIBILITIES

Over the past 50 years, the speed profiles of planes have changed significantly. The cruising speed of today's aircraft has increased several times, however, it is known that the higher the speeds of aircraft, the more difficult and persuasive are the conditions at low landing speeds.

Various witty inventions of constructors, such as changing the geometry of wings, developing a powerful takeoff – developing the mechanization of landing, enable the problem to be resolved to a certain degree, but everything has its limits. There are such unpleasant cases, such as the length of the landing distance (run-off) for the aircraft and the increased load on landing devices (wheels, brakes, tires or "pneumatics").

Any object in motion has a kinetic energy under the influence of the same movement. Its fundamental formula is: $K = MV^2/2$. An aeroplane, which, by itself, does not have a small mass M in the course of a landing at V_{nos}, has a very large kinetic energy supply. In order to stop an aircraft, this energy must be used (or transferred to other forms of energy that are not related to the movement of the aircraft). All braking techniques shall be directed directly to this.

In today's aviation, there are widely known three braking techniques: trust pulling back on the engines (reverse system), braking parachute (mostly used in past), and airplane wheel brakes. Alternatively, braking shuttles, braking shields and interceptors (mechanization of wings) may be mentioned.

4. CALCULATION ALGORITHM AND DEVICE DEVELOPMENT

4.1. Analytical establishment of parameters relationship

In order to create an algorithm for calculating the rest of the path it is necessary to take into account all of the above and to try to construct the relationship of values analytically, in deceleration and acceleration, depending on the time. Analytical analysis is entirely sufficient to construct a mathematical model, but real measurements can give a more accurate result.

The timing of the acceleration, as explained in the first chapter, should appear as a horizontal line in the idealized version (the run is a constantly accelerated movement of the plane).

The braking track may be divided into two steps (Fig. 4.2). The first phase is aerodynamic braking (frontal resistance, spoilers, reverse). The second phase is mechanical braking (aircraft wheel brakes).

Force kinetics that act on an aeroplane in the first phase:

$$a = \frac{dV}{dt} = \frac{1}{m}\sum F = -\frac{1}{m}\left(F_r - F_{sp} - F_{rev}\right) \tag{4.1}$$

where

F_r – wheel friction power;

F_{sp} – aerodynamic resistance;

F_{rev} – engines reverse trust.

These forces can be viewed in graphic form in Fig. 4.1. The graphs are designed analytically, so the accuracy and scale may be different in real circumstances.
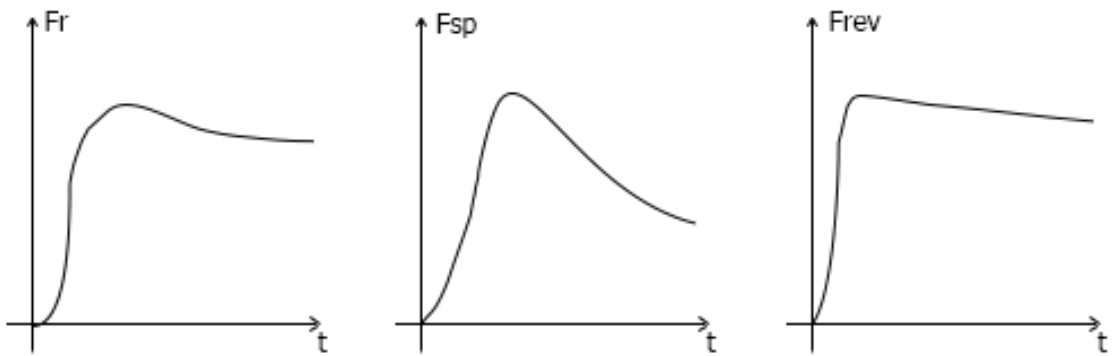

Fig. 4.1. Approximate representation of the braking force relationship over time.

As can be seen from the graphs in Fig. 4.1, the total braking path in the first phase will be permanently reduced, which gives us the possibility to predict that the acceleration (in our case marked with "–" mark), depending on the time in the first phase, is increasing rapidly and will gradually decrease until the braking is completed. The friction force of the wheels until the application of the brakes is insignificant and has only an informing nature.

The acceleration then rises even more rapidly as the brakes cause a very remarkable braking force. The forces that work in the first phase will get smaller as they lower the speed. Then the acceleration gradually reaches zero (the plane stops). The time-dependent acceleration is shown in Fig. 4.2.
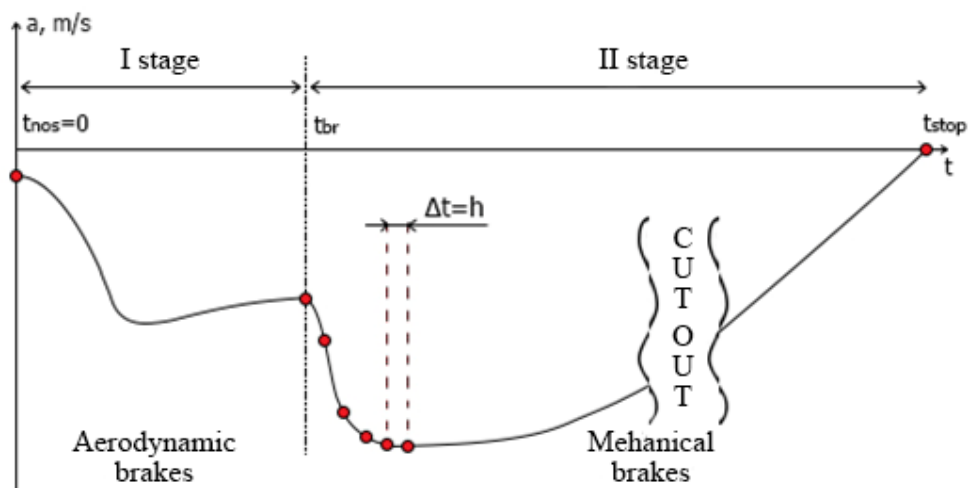
Fig. 4.2. Acceleration depending on time after landing: $t_{nos} = 0$ – calculation starting time from touchdown moment; t_{br} – start time of wheel braking application; t_{stop} – end time of braking, when speed $V = 0$; h – acceleration measurement interval.

4.2. Application of mathematical model

In order to predict the braking results, it is not possible to use formulas based solely on mechanical forces. These formulas are only applicable to uniformly slow motion (an ideal acceleration or braking pattern), using the mean values for the mechanical forces that act on the aeroplane at the moment of braking. These mean values can only be calculated after a complete transaction has been completed (takeoff/landing phases).

It will not be possible to apply these methods in real circumstances, since the result of braking should be predicted as early as possible in order to delay the time for correcting errors. Without it the time-dependent rate of acceleration will almost never be an analytical expression, this is why integrating the values analytically to find a stopping moment is not possible.

In this situation, the only option for forecasting at the author's discretion is the approximation (integration) of the accumulated statistics in the braking process. In particular, in this case, it is necessary to use the extrapolation of experimental points in M grade polynomial.

Extrapolation methods are similar to interpolation methods, only with the difference that the moments of interest are calculated beyond the experimental points and not between them.
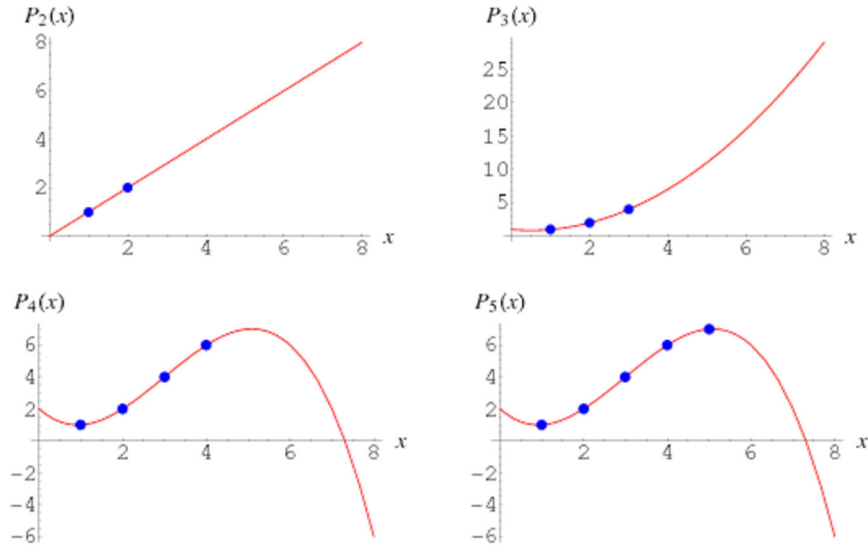
Fig. 4.3. Examples of extrapolation of experimental points.

Let us use the following terms. Let all measurements be numbered with index i, saying with 0 corresponding to the landing moment and ending with r corresponding to the last measurement executed. For all physical sizes, we adjust the appropriate measurement index. So, we have a set of arranged pairs at our disposal (t_i, a_i), where $i = 0, 1, 2, …, r$, and where it is the time at which i measurement was made, but the value of the acceleration obtained in this measurement (the corresponding deceleration value) is a_i). Our aim is to find acceleration as well as speed and coordinate at $t > t_r$. The mathematical model to be used is numerical extrapolation.

The time of the last measurement t_r is also the moment when we start extrapolation. In particular the most recent measurements $i = r$, r-1, must be taken into account. On the other hand, the information obtained in the earlier measurements ($i = 0, 1, ...$) may have a lower forecasting role as the braking forces tend to change dramatically (unlocking the reverse, changing wheel braking force, wind, etc.). We will examine the formulas that will be applicable using the last N measurements ($i = r$, r-1, …, r-N+1). Here N may have been selected as needed. If N is small ($6 ÷ 10$), only the most up-to-date information is used, if maximum, $N = r + 1$, then all measurements at our disposal ($i = 0, 1, 2, …, r$) are used. In addition, format does not change by choosing another N.

We choose the extrapolating function as an algebraic polynomial from time:

$$a(t) = \sum_{j=0}^{M} c_j t^j = c_0 + c_1 t + … + c_M t^M ,$$

(4.2)

where M is a polynomic grade.

This choice is justified because in a constant acceleration $a(t) = const,$ Formula (4.2) is applicable, selecting $M = 0$, which gives $a(t) = c_0$. The following members of the projection ($M = 1, 2, …$) shall comply with the adjustment for acceleration due to the variable forces. On the other hand, it would be inappropriate to use too much M. Really, in a border case where $M = N$–1, the polynomial will accurately describe all experimental values and will be heavily oscillated between experimental points and rapidly going to infinity beyond the experimental point range. The last such polynomial is not well suited for extrapolation purposes. A similar effect is expected if M is a little less than N but is approaching it.

As a result of these considerations, we can conclude that the optimal choice of M would be between $1 \div 4$. The final choice may be the result of the practical application of the method depending on how rapidly the acceleration (or speed) changes in reality.

So, look at the last N points $i = r, r-1, ..., r-N +1$. For convenience we will call it $k = i-r+N$. The new index changes to the following limits: $k = 1, 2 ,..., N$.

To find the best c_j value in Formula (4.2), look at the square deviation of the formula (4.2) from the experimental points (t_i, a_i):

$$\sum_{k=1}^{N}\left[a_i - a\left(t_i\right)\right]^2 = f\left(c_0, c_1, ..., c_M\right). \tag{4.3}$$

As shown clearly in Equation (4.3), this expression is a function of a c_j parameter. When equating to zero a derivative of this function after each parameter, get normal system of equations:

$$\sum_{j=0}^{M} c_j S_{l+j} = T_l \quad \left(l = 0, 1, ... M\right), \tag{4.4}$$

where

$$S_l = \sum_{k=1}^{N} t_k^l \quad un \quad T_l = \sum_{k=1}^{N} a_k t_k^l \tag{4.5}$$

in opened form:

$$\begin{cases} \sum_{j=0}^{M} c_j S_j = T_0 \\ \sum_{j=0}^{M} c_j S_{j+1} = T_1 \\ \qquad \dots \\ \sum_{j=0}^{M} c_j S_{j+M} = T_M \end{cases} \tag{4.6}$$

In Equation system (4.6) the values of S_l and T_l, $l = 0, 1, ..., M$, are known but the parameters c_j are unknown; they must have been found from these equations. The system (4.6) is a system of non-homogenic linear algebraic equations. Its handling techniques are well-designed. There are also standard programs in the packages of scientific programs (e.g., MATLAB) by which they can be resolved.

Once the parameters are found, we can use them in Equation (4.2), which will enable us to find the extrapolation formula for acceleration that we are looking for.

Now we can also get extrapolation formulas for speed and coordinates.

By integrating (4.2), we get:

$$V(t) = \int \sum_{j=0}^{M} c_j t^j = \sum_{j=0}^{M} \frac{c_j}{j+1} t^{j+1} + const. \tag{4.7}$$

Let us find a constant. If we know V_r at this point t_r:

$$V\left(t_r\right) = V_r \tag{4.8}$$

On the other hand, from Equation (4.7) it follows:

$$V\left(t_r\right) = \sum_{j=0}^{M} \frac{c_j}{j+1} t_r^{j+1} + const. \tag{4.9}$$

By aligning Equations (4.8) and (4.9), let us find a constant (*const*) and get:

29

$$V(t) = V_r + \sum_{j=0}^{M} \frac{c_j}{j+1}\left[t^{j+1} - t_r^{j+1}\right] \qquad (4.10)$$

Equation (4.10) is an extrapolation formula for speed. It gives an opportunity to find a stop time t_{stop}. When choosing times t_{r+1}, t_{r+2}, … (so that that it is $t_r < t_{r+1} < t_{r+2} < ...$), that let us tabling $V(t)$ forward until $V(t) = 0$ has been reached and $t = t_{stop}$. That means we have to solve the numerical equation $V(t_{stop})=0$.

We are now able to find the rest of the braking path until stopping (at moment t_r). Integrating (4.10) from t_r to t_{stop}. Let us get the rest of the way to stop:

$$S_{atl} = \int_{t_r}^{t_{stop}} V(t)\,dt = \left(V_r - \sum_{j=0}^{M} \frac{c_j}{j+1} t_r^{j+1}\right)\left(t_{stop} - t_r\right) + \sum_{j=0}^{M} \frac{c_j}{(j+1)(j+2)}\left[t_{stop}^{j+2} - t_r^{j+2}\right] \qquad (4.11)$$

After several attempts it was concluded that a number of data from AC systems were needed to extrapolate the acceleration. For the time being until such data exists it is proposed to extrapolate the directly measured speed for further development of the device.
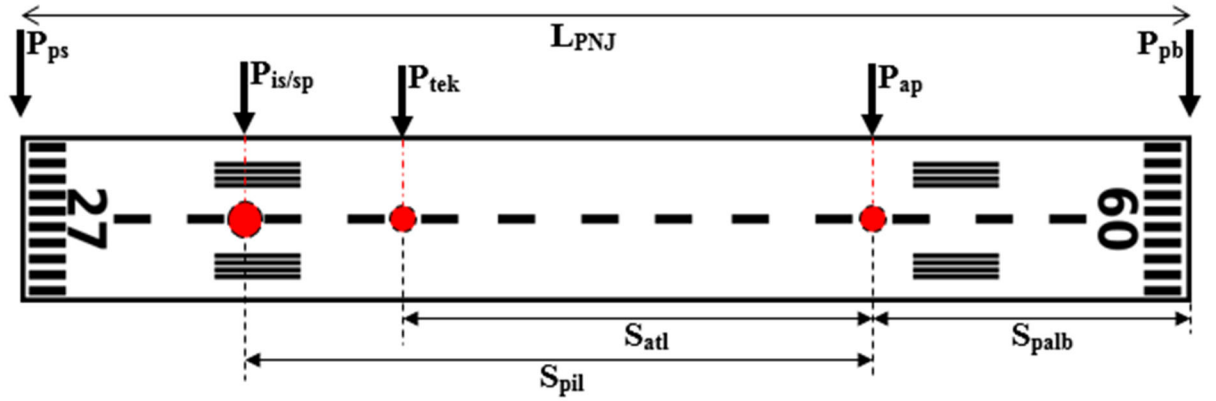
4.3. Algorithms

Fig. 4.4. Algorithm requires point and length terms.

In order to develop an algorithm, it is necessary to mark certain points on runway (PNJ).

During the development of the algorithm, the following expressions were invented (Fig. 4.4):

- P_{ps} – runway start point;
- P_{pb} – runway end point;
- $P_{is/sp}$ – AC acceleration/touchdown starting point;
- P_{tek} – AC current position on runway;
- P_{ap} – AC predicted rotate/stop point;
- S_{atl} –remaining path length of acceleration/braking;
- S_{pil} – remaining path length of acceleration/braking;
- S_{palb} – remaining runway length after rotate/stop point achieved against runway end point;
- L_{PNJ} – runway total length ($P_{pb} - P_{ps}$);

Calculation algorithm of takeoff runway length

1. Runway $P_{ps/pb}$ coordinates gated and saved to device memory data base.
2. Waiting for the start of the AC acceleration process.

30

3. Saving to memory starting speed V_{sak} and GPS coordinates ($P_{is/sp}$).
4. Writing acceleration value $a(t)$ with time interval Δh.
5. By integrating acceleration value $a(t)$, getting speed value $V(t)$ and saving it to memory.

$$V_t = \int a_i dt \qquad (4.12)$$

6. Performing $V(t)$ data approximation.

$$A(t) = aproks(V_t) \qquad (4.13)$$

7. Calculating the time left till liftoff, t_{atr} (predicting when v_2 speed is be achieved).

$$A(t_{atr}) = v_2 = v_{atr}, \qquad (4.14)$$

where t_{atr} is the estimated liftoff time when the speed function is equal to speed v_{atr} when AC leaves the ground.

8. By integrating speed $V(t)$, calculating the remaining ground path length S_{atl} till the liftoff point (when time is be t_{atr}).

$$S_{atl} = \int_{t_{tek}}^{t_{atr}} dt \int_{t_{tek}}^{t_{atr}} a_i dt \ . \qquad (4.15)$$

9. Current position P_{tek} can be calculated by integrating the speed from 0 to current time t_{tek}.

$$P_{tek} = \int_{t_0}^{t_{tek}} dt \int_{t_0}^{t_{tek}} a_i dt \ . \qquad (4.16)$$

10. Performing calculations, comparing it and providing relevant information to pilots about the predicted runoff point. In case the remaining runway length is not enough, warning the crew.

$$P_{ps} + P_{is/sp} + P_{tek} + S_{atl} < L_{PNJ} \ . \qquad (4.17)$$

11. Flying above the closest radio marker beacon (TRB), switching off the device calculation function, if necessary.

Calculation algorithm of the braking runway length

1. Runway $P_{ps/pb}$ coordinates given and saved to the device memory data base.
2. Flying above the closest radio marker beacon (TRB), switching on the device to standby mode.
3. Waiting for WOW condition (Weight on Wheel status from PSEU sensors).
4. Saving AC speed at touchdown moment V_{nos} and GPS coordinates ($P_{is/sp}$).
5. Writing acceleration value $a(t)$ with time interval Δh.
6. By integrating acceleration value $a(t)$, getting speed value $V(t)$ and saving it to the memory.

$$V_t = \int a_i dt \qquad (4.18)$$

7. Performing the speed integrated data approximation.

$$A(t) = aproks(V_t) \qquad (4.19)$$

8. Calculating the stop time when $V_{stop} = 0$.

$$A(t_{stop}) = V_{stop} = 0, \qquad (4.20)$$

where t_{stop} is estimated stop time when the speed is equal to 0.

9. By integrating speed *V(t),* performing calculation of the remaining ground path length till the stopping moment.

$$S_{atl} = \int\limits_{t_{tek}}^{t_{stop}} dt \int\limits_{t_{tek}}^{t_{stop}} a_i dt ,$$ (4.21)

where t_{tek} is current time; t_{stop} is estimated stop time.

10. Current AC position P_{tek} can be calculated by integrating the speed from 0 to current time.

$$P_{tek} = \int\limits_{t_0}^{t_{tek}} dt \int\limits_{t_0}^{t_{tek}} a_i dt$$ (4.22)

11. Performing calculations, comparing them and providing relevant information about the predicted stop position of AC. In case when the remaining runway length is not long enough, warning the crew.

$$P_{ps} + P_{is/sp} + P_{tek} + S_{atl} < L_{PNJ}$$ (4.23)

Graphic representation of electrical circuits

The development of an electrical scheme consisted of a rolled MultiSIM and NI Ultiboard software. Since it was not possible to select AVR's microcontrollers in the MultiSIM environment, a similar one was chosen – with 100 pines (ADSP-2111-PQFP (100)). Essentially, micro-controls differ mainly with the internal structure (memory, built-in functions, components, etc.), but the principle of operation is the same.

The list of the used components can be seen in Table 4.3.

Table 4.3

List of the Used Components

Quantity	Name
1	ATMega2650 MCU analogues
3	Couplers, HDR1X2, HDR1X3, HDR1X7
1	Transformer, T1
1	Diodes rectifier, 3N246
1	Capacitor, C1, 64 µF
1	LCD screen, GRAPH_LCD_M
1	Sound speaker, SONALERT
1	Fuse, F1
3	Light-emitting diodes, 3 colors
5	Different nominal resistances, R1-R5
1	Switch, S1

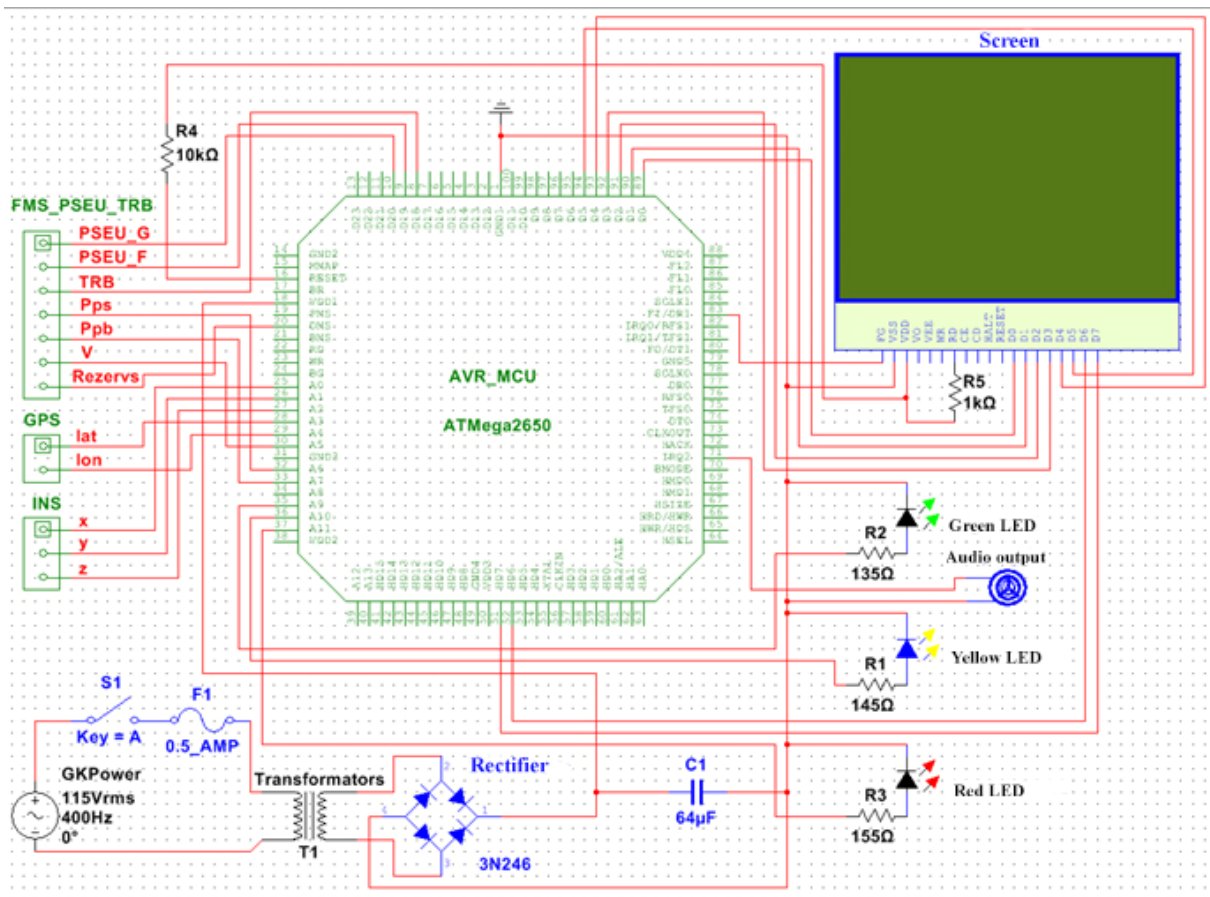The electrical diagram can be viewed in Fig. 4.5.

Fig. 4.5. Electrical diagram in MultiSIM software.

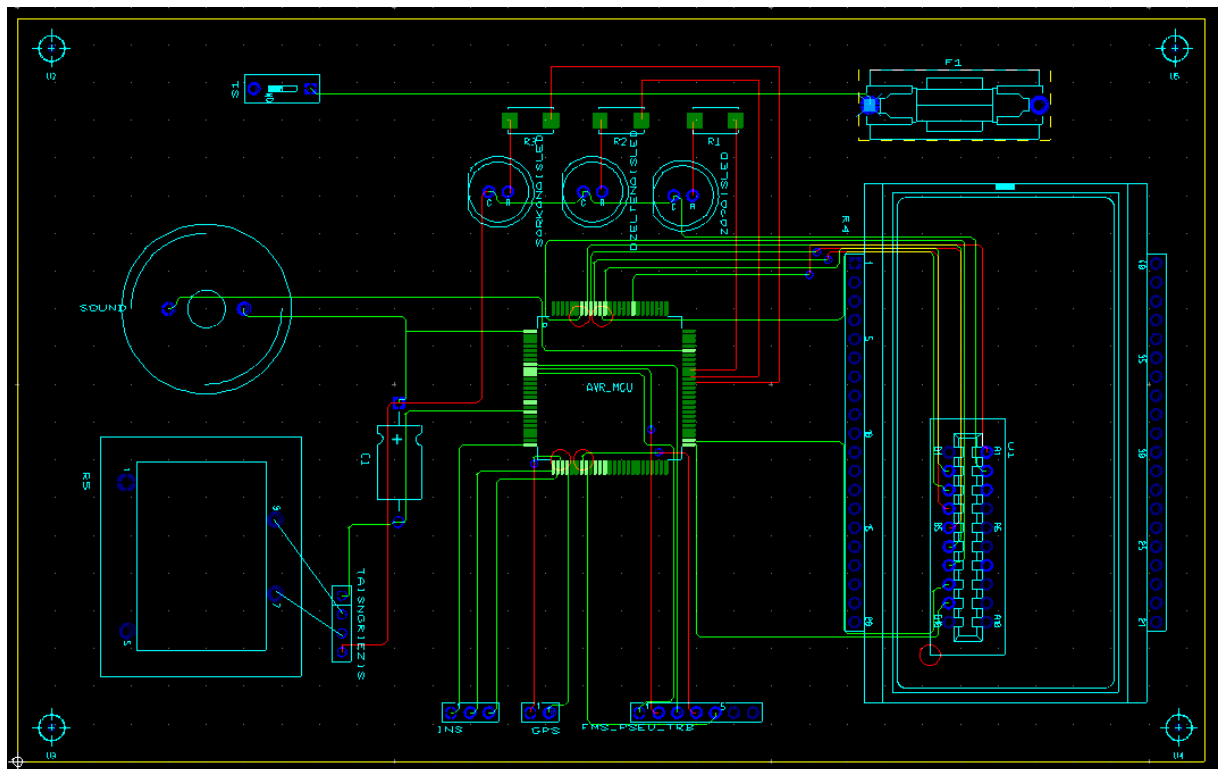Components location on board can be seen in Fig. 4.6.

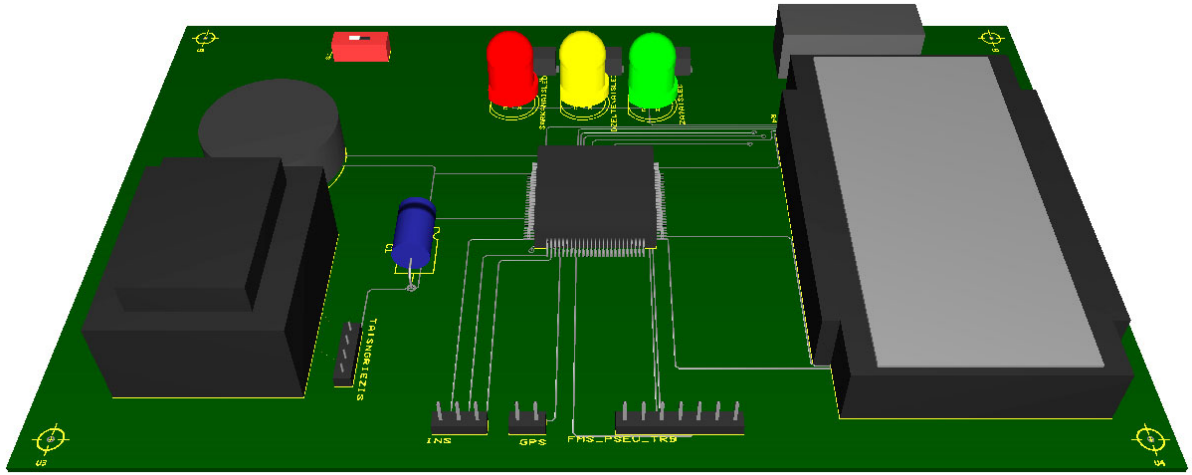Fig. 4.6. Electrical board in Ultiboard software.

Fig. 4.7. 3D view of printed circuit boards.

seethe figures show the dimensions of the mounting board, the list of parts, and their placement. In this case, the design of any other MCU device can also be considered as an electrical scheme to be used.

When designing a non-connectable (independent/portable) device, only the necessary components (accelerometer, GPS receiver, etc.) should be connected to inputs instead of AC system's exit data, as well as the power supply system recalculated if the power supply source is changed.
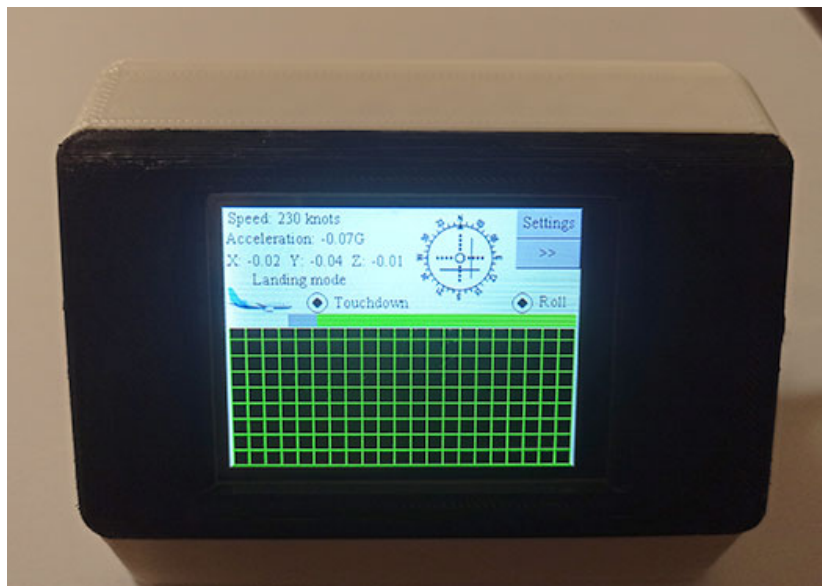

Fig. 4.8. Developed prototype with case.

5. PROTOTYPE APPLICATION, DATA OBTAINED, EXPERIMENT

5.1. Experiment 1: Analysis of a real flight for the probability of predicting runway adequacy by the end of runway.

A built device writes data in memory 10 times per second. The idea for the experiment is the following:

1) writing real data in memory;

2) after flight analysis of the data obtained;

3) comparing the modelling results with real data (received from sensors) by identifying an error between the remainder of the calculated runway path length and the data exactly on that flight.

Table 5.1

Example of Data from Sensors and Calculated Result

Time	Accel	Longitude	Latitude	V (km/h)	V (m/s)	S_{GPS} (m)	a_{TOTAL} (m/s^2)	S_{div} (a(V))	S_{APR} (m)	Error %
0	-0.09	E023 58.14	N56 54.67	207.05	57.51	0.00	0	0		
1	-0.13	E023 58.15	N56 54.70	204.83	56.90	52.33	-0.612398926	57.2038		
2	-0.11	E023 58.15	N56 54.73	202.79	56.33	104.77	-0.589144134	113.8417	2322.724	56.96
3	-0.16	E023 58.17	N56 54.76	195.57	54.33	167.01	-1.061541069	167.7531	2294.305	55.04
4	-0.23	E023 58.17	N56 54.76	188.16	52.27		-1.310600658	219.5552	2115.666	42.97
5	-0.13	E023 58.17	N56 54.79	180.57	50.16	224.62	-1.470325308	269.1709	1952.869	31.97
6	-0.11	E023 58.17	N56 54.81	172.98	48.05	263.63	-1.576808408	316.6774	1930.008	30.42
7	-0.13	E023 58.17	N56 54.84	165.57	45.99	315.34	-1.645518553	362.2548	1891.264	27.80
8	-0.11	E023 58.18	N56 54.87	160.75	44.65	373.64	-1.607023312	408.6553	1841.704	24.45
9	-0.12	E023 58.18	N56 54.90	156.49	43.47	425.99	-1.559934408	454.4127	1793.821	21.22
10	-0.17	E023 58.20	N56 54.93	152.05	42.24	488.24	-1.527407732	498.7296	1754.231	18.54
11	-0.12	E023 58.20	N56 54.93	147.60	41.00		-1.500794998	541.8119	1725.416	16.60
12	-0.12	E023 58.20	N56 54.96	143.16	39.77	545.85	-1.478617719	583.6595	1701.211	14.96
13	-0.14	E023 58.21	N56 54.99	138.90	38.58	600.50	-1.455895062	624.6069	1689.989	14.20
14	-0.12	E023 58.21	N56 54.99	134.46	37.35		-1.440093104	664.0109	1680.442	13.56
15	-0.13	E023 58.21	N56 55.02	130.01	36.11	656.19	-1.426398074	702.1802	1644.790	11.15
16	-0.11	E023 58.21	N56 55.05	125.75	34.93	706.59	-1.411199642	739.5264	1618.410	9.36
17	-0.10	E023 58.21	N56 55.05	121.31	33.70		-1.400815408	775.2522	1591.578	7.55
18	-0.07	E023 58.21	N56 55.08	116.86	32.46	770.09	-1.391584977	809.7432	1565.137	5.76
19	-0.07	E023 58.21	N56 55.11	112.42	31.23	821.80	-1.383326171	842.9996	1541.368	4.16
20	-0.07	E023 58.21	N56 55.11	110.38	30.66		-1.342454329	881.7091	1543.629	4.31
21	-0.02	E023 58.23	N56 55.14	108.53	30.15	879.11	-1.303025307	920.3929	1564.689	5.73
22	0.01	E023 58.23	N56 55.14	106.86	29.68		-1.264842355	959.1282	1599.895	8.11
23	-0.02	E023 58.23	N56 55.17	105.01	29.17	938.20	-1.232216377	996.8088	1633.684	10.40
24	-0.04	E023 58.23	N56 55.17	103.16	28.65		-1.20230923	1033.975	1653.185	11.71
25	0.00	E023 58.24	N56 55.20	101.30	28.14	994.30	-1.174794655	1070.627	1647.967	11.36
26	-0.02	E023 58.24	N56 55.20	100.38	27.88		-1.139503416	1110.108	1650.242	11.52
27	-0.02	E023 58.24	N56 55.22	99.45	27.63	1030.00	-1.106826342	1149.332	1658.367	12.06
28	-0.03	E023 58.24	N56 55.22	98.53	27.37		-1.076483345	1188.299	1669.728	12.83
29	-0.04	E023 58.24	N56 55.25	97.60	27.11	1080.00	-1.048232969	1227.008	1679.916	13.52
30	-0.07	E023 58.24	N56 55.25	96.86	26.91		-1.020151134	1266.232	1687.497	14.03
31	-0.12	E023 58.24	N56 55.28	95.93	26.65	1140.00	-0.995540531	1304.453	1686.421	13.96
32	-0.11	E023 58.24	N56 55.28	95.01	26.39		-0.97246809	1342.416	1684.874	13.86
33	-0.11	E023 58.26	N56 55.31	90.75	25.21	1200.00	-0.978854608	1364.844	1656.216	11.92
34	-0.13	E023 58.26	N56 55.31	85.93	23.87		-0.989404667	1383.464	1610.513	8.83
35	-0.12	E023 58.26	N56 55.34	81.30	22.58	1250.00	-0.997882023	1401.647	1564.167	5.70
36	-0.14	E023 58.26	N56 55.34	76.49	21.25		-1.007317429	1417.618	1526.232	3.14
37	-0.15	E023 58.27	N56 55.34	71.77	19.93		-1.015547617	1432.728	1502.381	1.52
38	-0.13	E023 58.27	N56 55.37	67.04	18.62	1310.00	-1.023344637	1446.525	1494.569	1.00
39	-0.13	E023 58.27	N56 55.37	62.30	17.31		-1.030873719	1458.911	1489.550	0.66
40	-0.14	E023 58.27	N56 55.37	57.43	15.95		-1.038926625	1469.259	1484.211	0.30
41	-0.14	E023 58.27	N56 55.37	52.84	14.68		-1.044704592	1479.836		

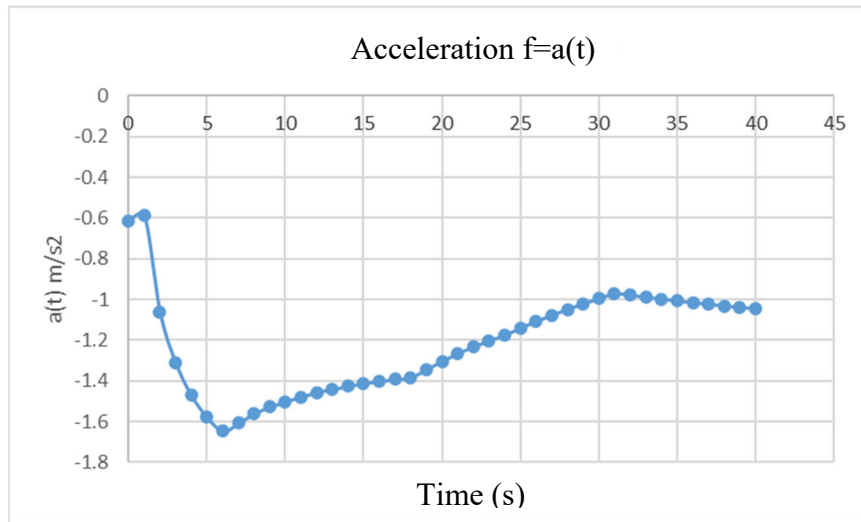Graphical view of data is shown in the following figures.

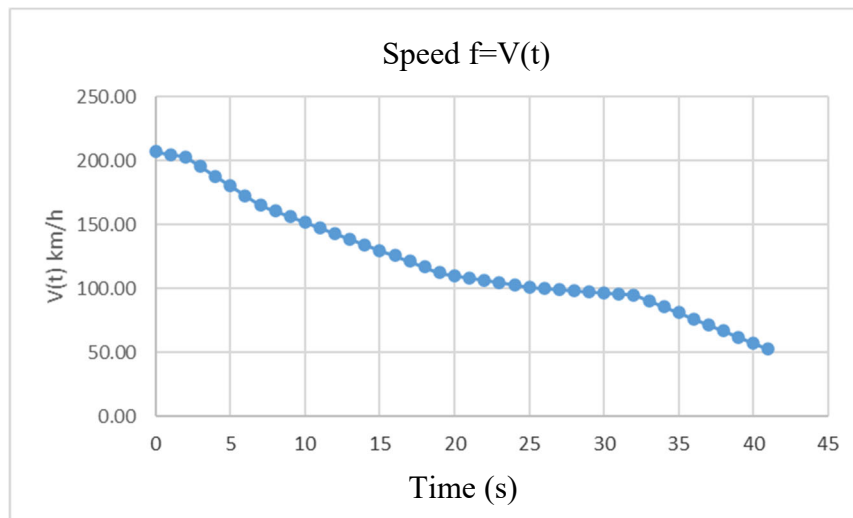Fig. 5.1. Acceleration changes during the time.
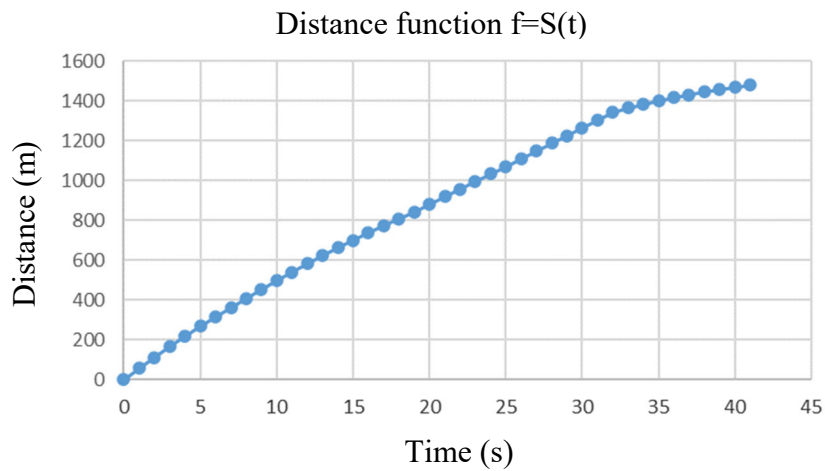

Fig. 5.2. Speed changes during the time.

Fig. 5.3. Distance changes during the time.

Fig. 5.4. Data on braking path received from GPS receiver.

Figure 5.5 shows the predicted path to stop/liftoff point (a blue line – actual data obtained; red line – calculated or predictable data, drawn by interpolation).
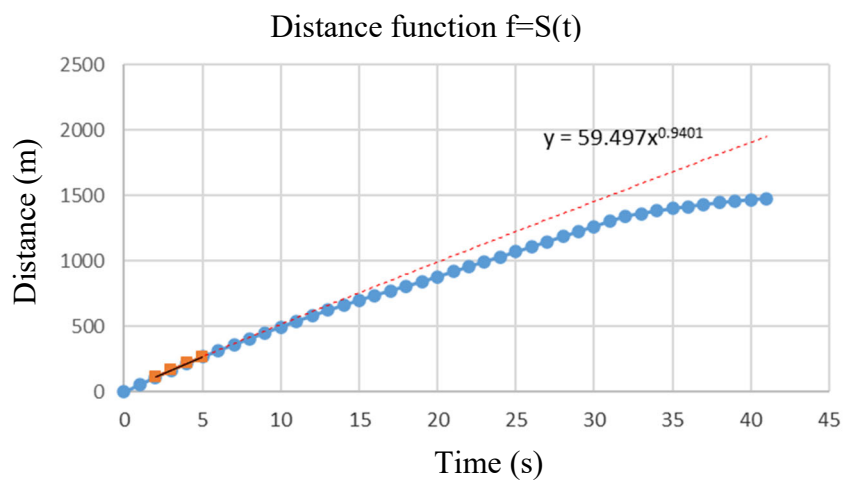

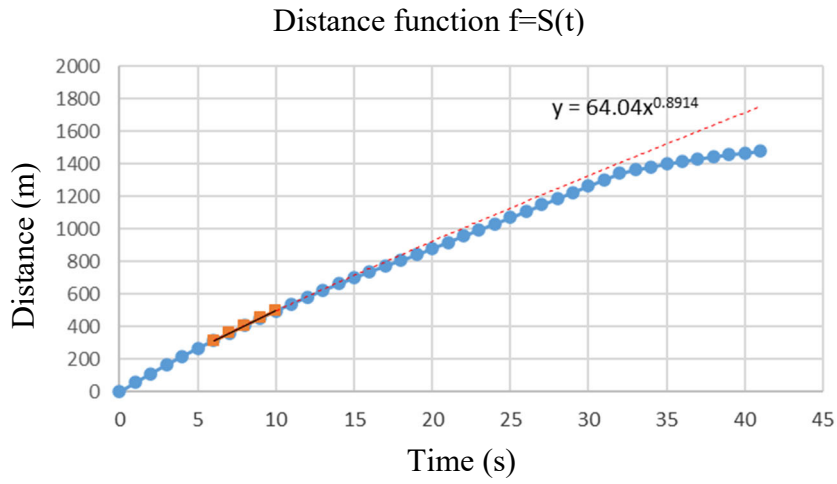Fig. 5.5. Interpolated predicted distance at the 5th second S5s = 1952.869 m.

Fig. 5.6. Interpolated predicted distance at the 10th second S10s = 1754.231 m.
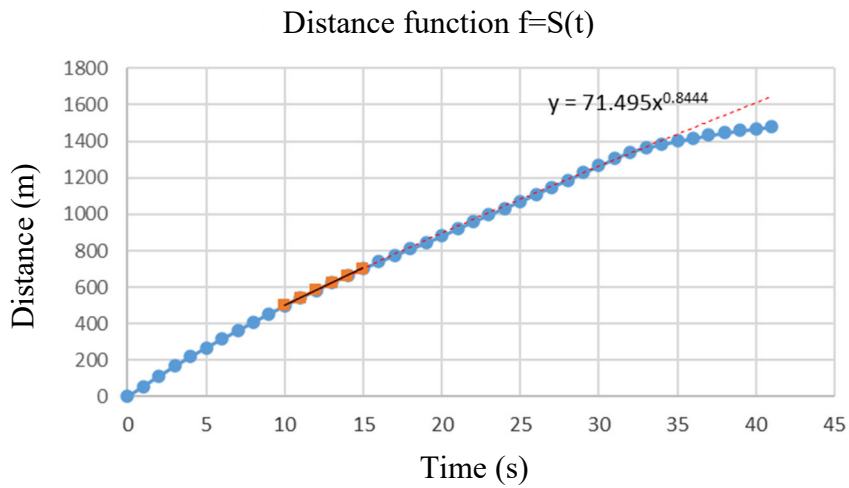

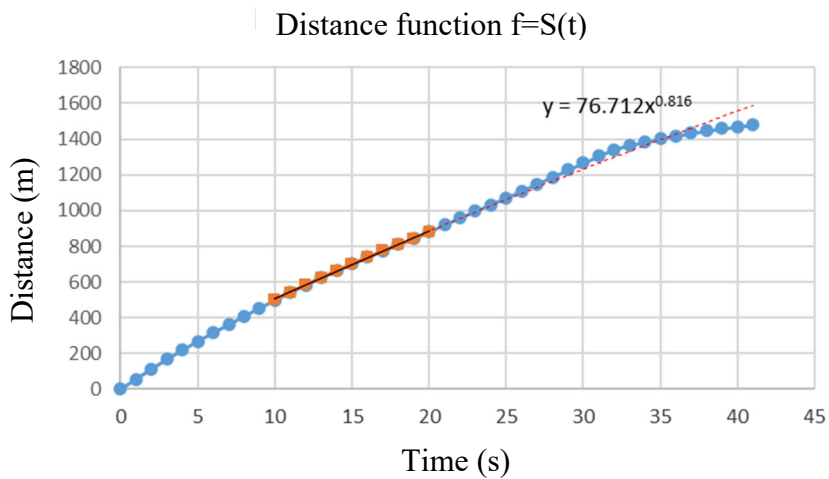Fig. 5.7. Interpolated predicted distance at the 15th second S15s = 1644.79 m.

Fig. 5.8. Interpolated predicted distance at the 20th second S20s = 1588.162 m.

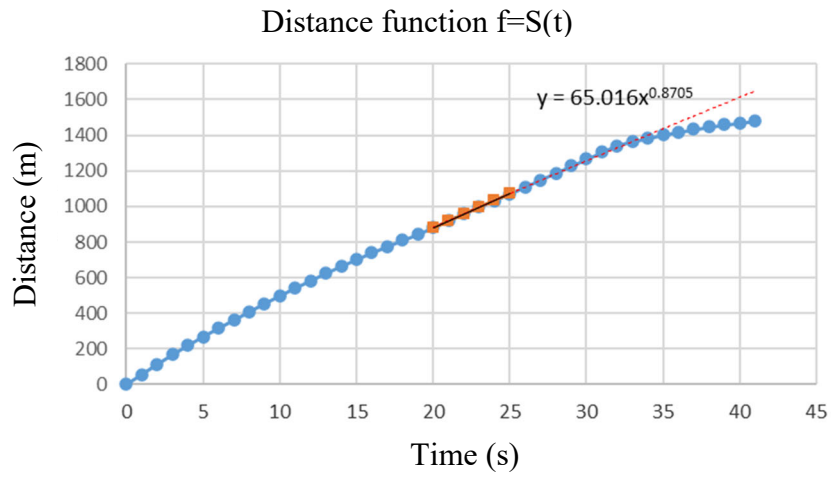Fig. 5.9. Interpolated predicted distance at the 25th second S25s = 1647.967 m.

Fig. 5.10. Interpolated predicted distance at the 30th second S30s = 1687.497 m.

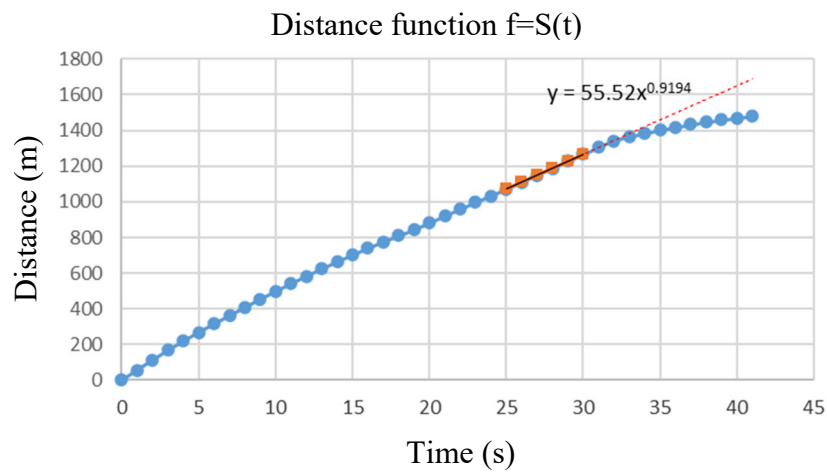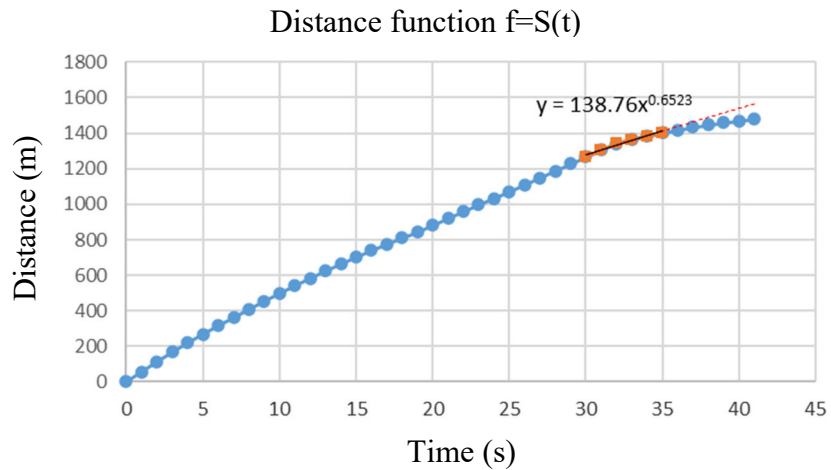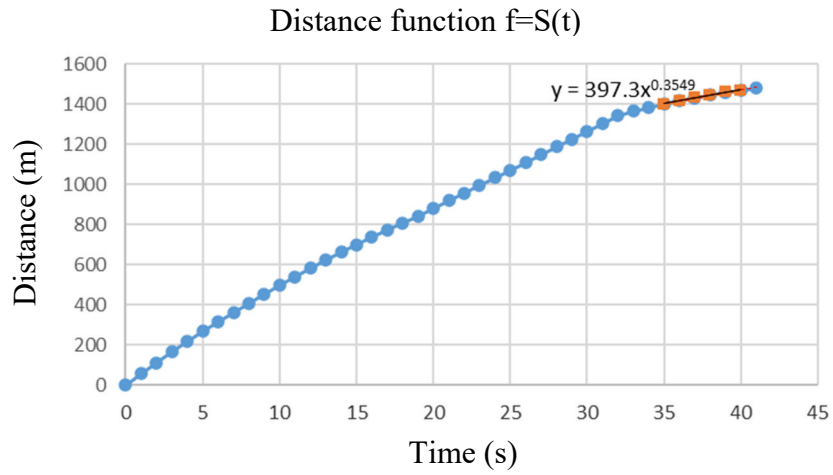Fig. 5.11. Interpolated predicted distance at the 35th second S35s = 1564.167 m.

Fig. 5.12. Interpolated predicted distance at the 40th second S40s = 1484.211 m.

The results of another experiment are shown in Fig. 5.13: received data (blue color) and forecasts (red color).
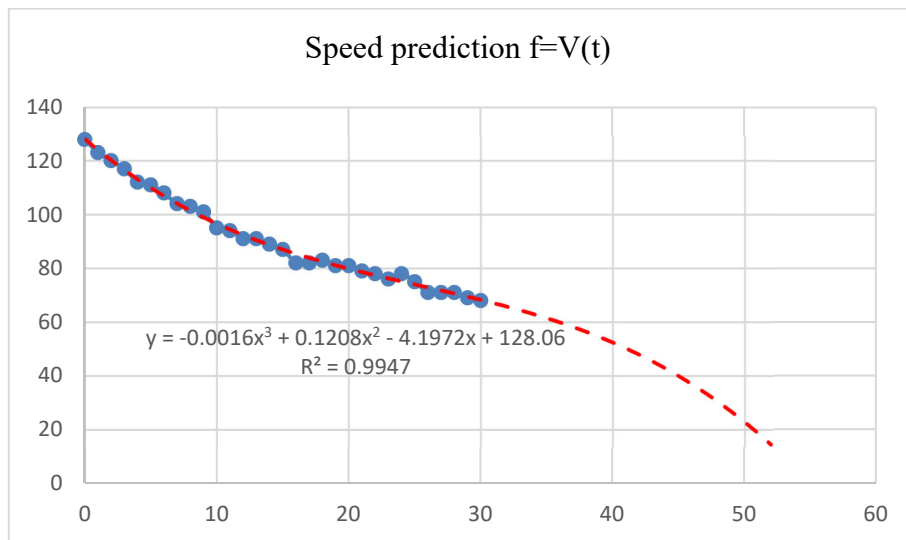

Fig. 5.13. Example of speed forecasting at the braking phase.
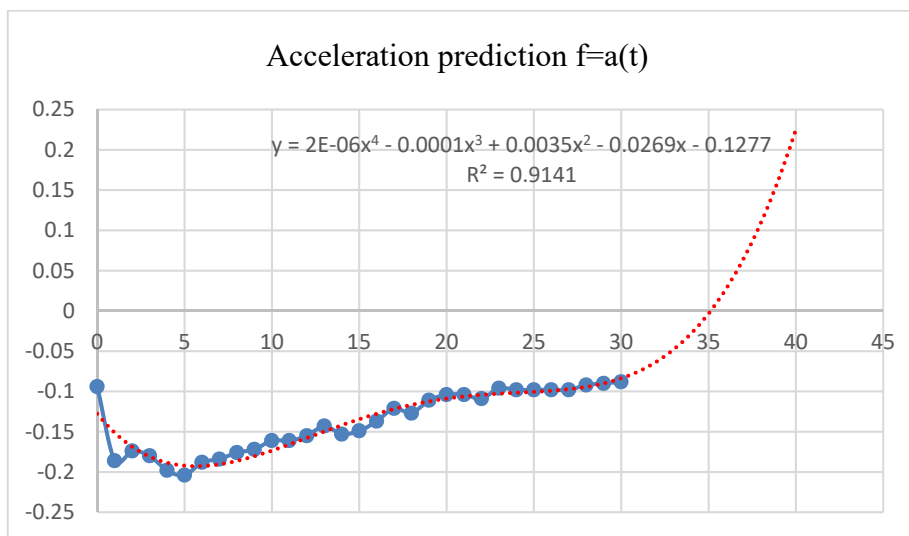

Fig. 5.14. Example of acceleration forecasting at the braking phase.
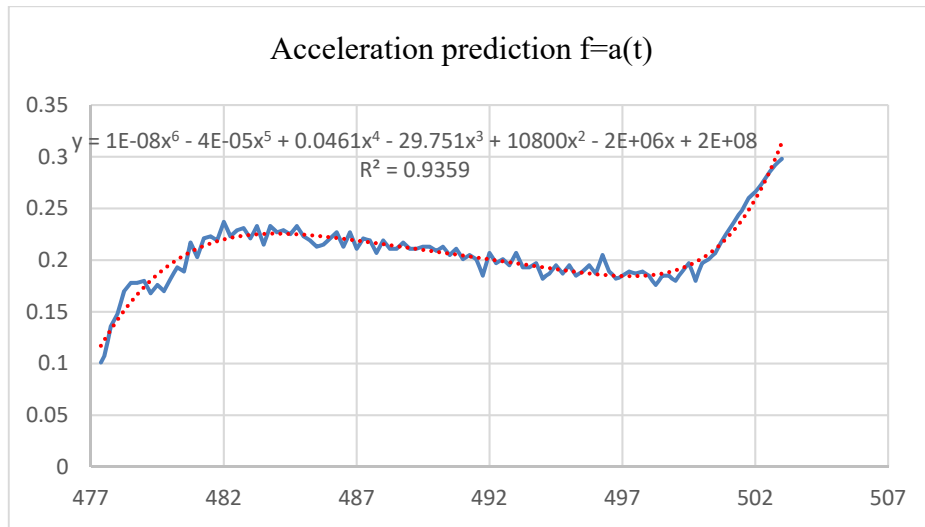
Fig. 5.15. Example of acceleration forecasting in the takeoff phase.
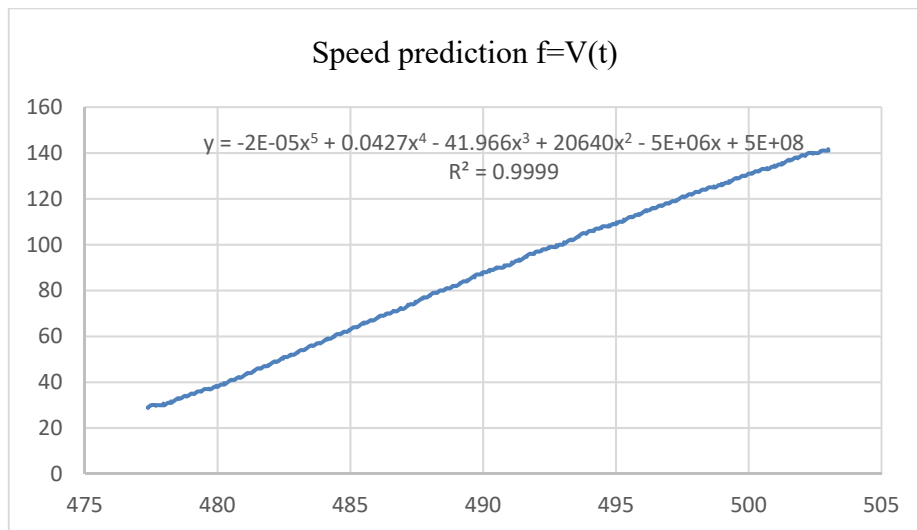
Fig. 5.16. Example of speed forecasting in the takeoff phase.

5.2. Experiment 2: Analysis of the probability of the main objective of the Thesis

The above described experiment shows that the device is workable to calculate the path and may in practice be used to predict the result of takeoff/landing phases. In case the remaining distance is sufficient, no more braking forces will be needed to be applied. A number of incidents linked to the runway excursion are associated with pilot errors and technical problems. The main advantage of injecting such type of device is that it can predict a problem more quickly than a person can do, and do so at a time a person cannot calculate in order to act accordingly. It must be understood, of course, that in some cases it will not be enough to know whether there is enough runway or not; in some cases additional devices will have to be used to correct and timely brake an aircraft with which several aircraft are not equipped today. The idea developed in the Thesis is only the first step that will help to apply it in the future and will lead ancillary systems to increase flight safety significantly.

The proposed method can also be used at daily bases. It is about the takeoff/landing phases where it is known that it is possible to brake/liftoff in time (according to distance) by

increasing the length of the runway (by lowering the braking and engine power usage). The result of the previous experiment, e.g., with an "error" of 56.96 %, shows that if the braking forces at this moment do not change further, the plane will stop at 2322 m, and if the runway length is 3.2 km nothing more can be done (stopping will happen before the end of the runway), and, on the contrary, if the runway length is not enough, braking must be more intensive. It should be noted that pilots did not control the process according to the method proposed in this work and the acceleration changed significantly over time, as demonstrated by the results of the experiment, which also changes the estimated result.

In Experiment 2, we will carry out a test for the main task, try to reach the prescribed speed at the specified point and brake to a certain speed at the specified point. The realization of this experiment with real aircraft means to violate the flight safety rules, therefore it was decided to perform experiments with a conventional car on normal roads.
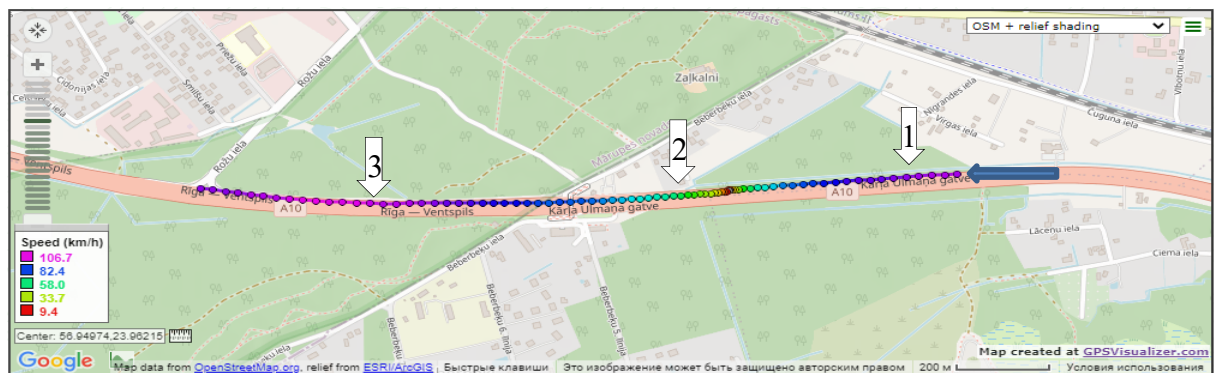
Fig. 5.17. Experimental runway trajectory.

The idea of the experiment is shown in Fig. 5.17:

1. Loading the program into the device to brake from 100 km/h to 0–10 km/h and accelerate immediately to 100 km/h. The point where the brake is to be started is marked with "1" (E23 .974497, N56 .950203), the starting point of stopping and following acceleration "2" (E23 .966328, N56 .949825) at a speed of 0–10 km/h. Speed 100 km/h required to be achieved at point "3" (E23 .955357, N56 .949533). The length of the road from 1 to 2 must be equal to 500 meters, from 2 to 3 to 700 meters.

2. The task is to reach 100 km/h speed before point "1" and hold it.

3. The device issues an audible signal at the "1" point, which means that the process has started and should be braked by operator according to the instructions of the device on the right side of the screen (try to keep the diamond in the center on the lower side).

4. At the "2" point, the device issues two audible signals and waits for acceleration to begin by putting the diamond at the top, which means the need to increase acceleration.

5. When accelerating from point "2" to point "3", the operator should try to keep the diamond in the center of the upper side of the indicator).

Results:

Table 5.2

Data from Experiment 2

Time	Longitude	Latitude	a_{TOTAL} (m/s²)	V (km/h)	V (m/s)	Rec	L (km)
1	23.974497	56.950203	0.29313	100.10	27.81	-1	0.000
2	23.974037	56.950180	0.30113	101.20	28.11	-3	0.028
3	23.973573	56.950160	0.26168	102.00	28.33	-5	0.056
4	23.973120	56.950140	-0.04777	99.60	27.67	-5	0.084
5	23.972670	56.950122	-0.09138	98.80	27.44	-6	0.112
6	23.972227	56.950100	-0.15088	97.40	27.06	-4	0.139
7	23.971800	56.950085	-0.29703	93.70	26.03	-5	0.165
8	23.971375	56.950063	-0.26254	93.50	25.97	-6	0.191
9	23.970952	56.950042	-0.24708	93.00	25.83	-5	0.216
10	23.970533	56.950022	-0.24741	92.10	25.58	-3	0.242
11	23.970132	56.950005	-0.33378	88.10	24.47	-4	0.267
12	23.969737	56.949988	-0.33626	86.80	24.11	-3	0.291
13	23.969350	56.949972	-0.34991	85.00	23.61	-4	0.314
14	23.968972	56.949955	-0.36359	83.10	23.08	-4	0.337
15	23.968608	56.949942	-0.40111	79.90	22.19	-4	0.360
16	23.968255	56.949925	-0.41696	77.60	21.56	-6	0.381
17	23.967928	56.949908	-0.48812	72.00	20.00	-7	0.401
18	23.967630	56.949895	-0.56562	65.50	18.19	-6	0.419
19	23.967345	56.949883	-0.57895	62.60	17.39	-5	0.437
20	23.967087	56.949873	-0.63474	56.70	15.75	-5	0.452
21	23.966867	56.949860	-0.71689	48.50	13.47	-5	0.466
22	23.966688	56.949852	-0.80444	39.30	10.92	-4	0.477
23	23.966555	56.949847	-0.89540	29.20	8.11	-3	0.485
24	23.966445	56.949842	-0.91686	24.20	6.72	-4	0.492
25	23.966377	56.949838	-0.98514	15.00	4.17	-5	0.496
26	23.966338	56.949833	-1.01462	8.80	2.44	-5	0.498
27	23.966328	56.949825	-1.05893	1.00	0.28	0	0.499
28	23.966328	56.949825	-0.00342	0.00	0.00	0	0.499
29	23.966328	56.949825	0.00210	0.00	0.00	0	0.499
30	23.966328	56.949825	0.00420	0.00	0.00	0	0.499
31	23.966328	56.949825	0.03245	0.00	0.00	0	0.499
32	23.966328	56.949825	0.04235	0.00	0.00	0	0.499
33	23.966242	56.949802	0.05389	5.20	1.44	7	0.505
34	23.966173	56.949795	0.13811	15.40	4.28	7	0.509
35	23.966085	56.949787	0.16755	19.50	5.42	6	0.515
36	23.965962	56.949777	0.22387	27.20	7.56	5	0.522
37	23.965825	56.949763	0.24312	30.50	8.47	6	0.531
38	23.965667	56.949758	0.26808	34.70	9.64	7	0.541
39	23.965492	56.949752	0.28807	38.40	10.67	5	0.551
40	23.965312	56.949742	0.28923	39.60	11.00	5	0.562
41	23.965103	56.949733	0.32575	45.90	12.75	5	0.575
42	23.964877	56.949725	0.34287	49.60	13.78	5	0.589
43	23.964622	56.949713	0.37770	56.10	15.58	5	0.604
44	23.964350	56.949702	0.39282	59.80	16.61	5	0.621
45	23.964072	56.949688	0.39273	61.20	17.00	4	0.638
46	23.963775	56.949673	0.40931	65.30	18.14	5	0.656
47	23.963468	56.949653	0.41490	67.70	18.81	6	0.675
48	23.963167	56.949642	0.39662	66.10	18.36	7	0.693
49	23.962845	56.949627	0.41556	70.80	19.67	6	0.713
50	23.962515	56.949612	0.41671	72.50	20.14	5	0.733
51	23.962172	56.949600	0.42393	75.30	20.92	4	0.754
52	23.961820	56.949592	0.42597	77.20	21.44	5	0.775
53	23.961425	56.949580	0.46853	86.70	24.08	5	0.800
54	23.961050	56.949577	0.43610	82.20	22.83	5	0.822
55	23.960668	56.949565	0.43626	83.80	23.28	6	0.846
56	23.960273	56.949553	0.44297	86.70	24.08	6	0.870
57	23.959888	56.949538	0.42464	84.60	23.50	5	0.893
58	23.959510	56.949537	0.40842	82.80	23.00	4	0.916
59	23.959122	56.949533	0.41192	85.00	23.61	5	0.940
60	23.958720	56.949532	0.41953	88.10	24.47	4	0.964
61	23.958320	56.949527	0.41069	87.70	24.36	4	0.989
62	23.957918	56.949535	0.40577	88.10	24.47	5	1.013
63	23.957515	56.949542	0.40013	88.30	24.53	6	1.038
64	23.957098	56.949543	0.40744	91.40	25.39	5	1.063
65	23.956673	56.949545	0.40846	93.10	25.86	5	1.089
66	23.956240	56.949543	0.40986	94.90	26.36	5	1.115
67	23.955802	56.949542	0.40828	96.00	26.67	5	1.142
68	23.955357	56.949533	0.40882	97.60	27.11	5	1.169
69	23.954897	56.949527	0.41588	100.80	28.00	5	1.197
70	23.954435	56.949523	0.41147	101.20	28.11	5	1.225
71	23.953962	56.949523	0.41511	103.60	28.78	5	1.254
72	23.953488	56.949535	0.41083	104.00	28.89	5	1.283
73	23.953010	56.949545	0.40821	104.80	29.11	5	1.312
74	23.952532	56.949553	0.40262	104.80	29.11	5	1.341
75	23.952053	56.949565	0.39793	105.00	29.17	5	1.370
76	23.951572	56.949588	0.39559	105.80	29.39	5	1.400
77	23.951087	56.949605	0.39294	106.50	29.58	5	1.429
78	23.950608	56.949622	0.38315	105.20	29.22	5	1.458
79	23.950148	56.949653	0.36506	101.50	28.19	5	1.487
80	23.949693	56.949692	0.35833	100.90	28.03	5	1.515
81	23.949238	56.949725	0.35281	100.60	27.94	5	1.542
82	23.948795	56.949768	0.34159	98.60	27.39	5	1.570
83	23.948347	56.949793	0.33776	98.70	27.42	5	1.597
84	23.947887	56.949833	0.34474	102.00	28.33	5	1.626
85	23.947440	56.949875	0.33204	99.40	27.61	5	1.653

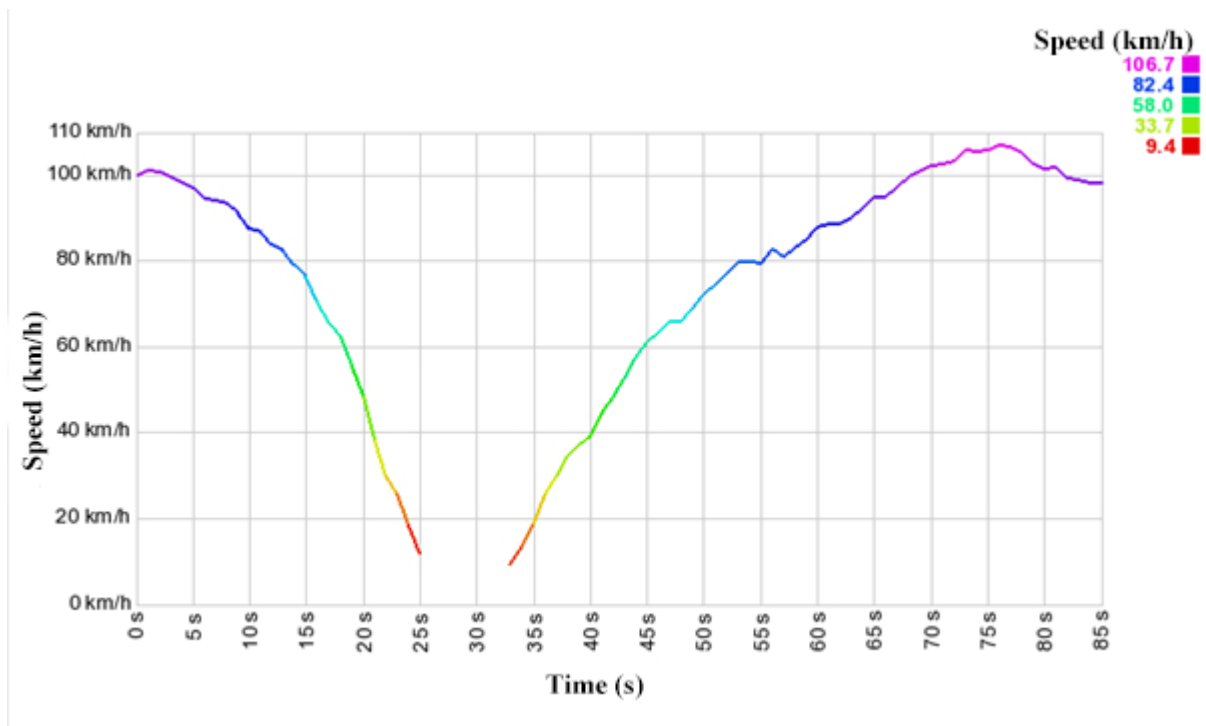Graphical view of speed is shown in Fig. 5.18.

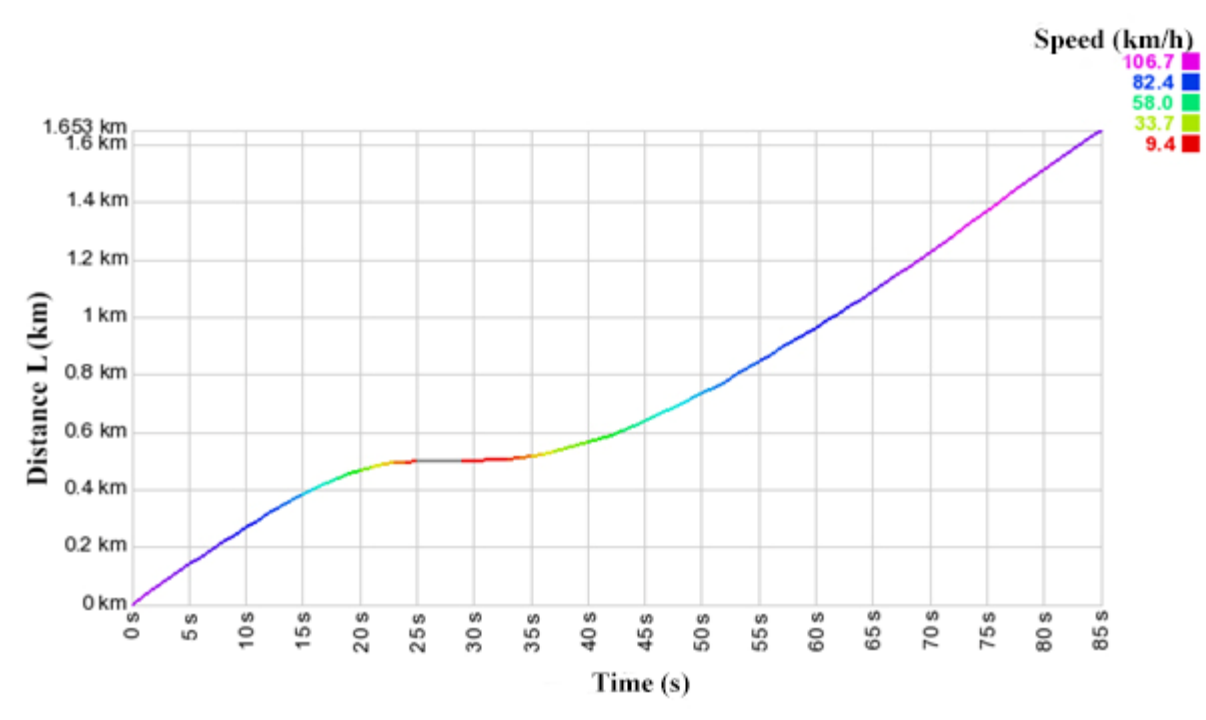Fig. 5.18. Graphical view how speed changes during time.

Fig. 5.19. Graphical view of distance changes during time.

Result: In this experiment, braking and accelerating following the recommendations of the device, succeeded in stopping at the specified point with an accuracy of 1 meter (the 27th second in Table 5.2) and achieving the required speed at the specified point (3) with an accuracy of 3 meters. It should be noted that the GPS receiver had an error of ±2 meters at this time and that the speed was calculated with a specified delay (0.5 sec.). When performing a series of tests (varying speeds, distance lengths and braking/acceleration style) and taking into account the

44

above, the average total error of the error was ±3.7 meters. There is a human factor in this experiment as well, which affects the calculation of the error, because there is a slight delay between the moment when the device refers to what to do with the braking/acceleration factor and the moment when the operator realize it and how correctly it has been done. Thus, it can be concluded that by connecting the device to the sensors and input organs of research transport, the accuracy of the system can be further increased. The speed value, distance length and vehicle length/mass, which will have an impact on the result, must be recognized. Taking into account the principle of sensory action we understand that the greater is the vehicle (length, mass) and the higher the speed the higher accuracy will be achieved, and the permitted deviation from this result will be higher (permissible error).

In experiments when the weather was bad (a low coefficient of friction with asphalt) with shorter distances and without following the recommendations of the device to change the required acceleration, it is evident in a very rapid response of the device to the situation. In all cases, the device correctly calculated that it would not be possible to reach the prescribed speed at the specified point.

Overall, the result of the experiment shows that the use of this methodology during the acceleration and braking phases can achieve scheduled promotion targets, i.e., to accelerate AC safely during takeoff with reduced engine power (if it is allowed by the runway length and other conditions) and to brake down to the roll path (specified point on runway) in such a way that it is not necessary to apply engine power then to speed up again after fast braking to achieve the specified point (rollout way). As a result, we can use the AC resources more efficiency and economically, decrease pollutions and increase safety.

MAIN RESULTS AND CONCLUSIONS

As a result of the development of the promotion work, the braking methods, landing and takeoff phases, factors that affect the length of these stages, as well as the current situation and modern solutions of the problem were examined. An analysis was carried out of the need to create a system capable of controlling the takeoff and landing processes and showing the remaining length of the runway until the stop or exit/liftoff points against the end of the runway. The calculation is based on the results of inertial navigation system data integration. A portable device has been developed that can also be very useful in flight quality analysis and flight accident investigations, especially with light aircraft and aircraft that are poorly equipped with modern flight and navigation equipment.

In order to predict the time until the plane stops or liftoff, the method of matching the result of the acceleration integration with corrective factors accumulated in the acceleration statistics shall be used. This task may also be resolved by other methods mentioned in this work. However, different other methods are very difficult to implement, particularly in the software, and it was decided to avoid using them in the cases with a rather high degree of accuracy for the current algorithm. Which one from the methods will produce the best results, can only be found in a practical way by conducting a series of tests for each specific type of aircraft. This method can be applied not only in aviation but also in other transport (cars, ships, etc.), where it is necessary to forecast distances and/or optimize them.

As part of the development of the device, an electrical circuit was designed, its elements calculated and selected, and the program was written in C++ programming language to organize the microcontroller. As a result, a fully operational device was assembled, which can be connected at any time to the systems mentioned in this work. As the device is not certified, it can currently only be used as a portable accessory without connecting to the aircraft equipment. The main task of the Thesis was to display a new method not a finished product. The device has been built for obtaining the data on these processes, as they are not available anywhere, and to display the practical application of the algorithm.

The data received during the takeoff/landing phases in real flight by using a designed prototype proved that it is possible to calculate the liftoff/stop points dynamically over time during the whole phase. Taking into account the nature of the counting algorithm (acceleration control), the method makes it possible to control absolutely all the factors that affect the travel length (e.g., a sudden change in the wind parameter or runway position will lead to a change in acceleration). Although the number of tests does not allow conclusions on how the method increases the safety of takeoff/landing stages, it clearly proposes solutions for achieving the following advantages and opportunities:

1. To significantly lower the economic component and prolong the longevity of the AC resources compared to the standard takeoff/landing method (the maximum permitted use of propulsion power during the takeoff phase and the selection of maximum speed braking styles at the landing stage, which then most often requires the acceleration of the plane to the rollout route).

2. The reduction of fuel consumption, tires/brakes usage and other AC resources leads to a reduction in environmental pollution.

3. It is possible to have better orientation on the entire runway (not only bad weather conditions, but also a person who is unable to see the whole length of the runway and to

understand/calculate the passed and the remaining length of the runway) and to be sure that the aircraft is on the correct runway (another rather current problem – there have been a number of cases when the takeoff phase was performed from the taxi way).

4. To increase the safety of the takeoff/landing phases (mainly without the maximum engine power being used, which significantly reduced the probability of engine failure) and increase the safety of the takeoff/landing phases at aerodromes not equipped with ILS and similar systems (e.g., "Spilve airport") or non-certified aeroplanes (for experimental purposes) not equipped with appropriate systems.

5. It can facilitate the crew operation by providing additional information about acceleration/braking progress and location on the runway.

6. To allow perform landing by ILS Category I rules at airports not equipped with course-to-approach systems with a GPS receiver embedded in the device, as well as landing on complex approach trajectories (e.g., mountain areas). Such systems already exist, therefore this function is not described due to the lack of novelty.

7. Lowering the weather requirements for aeroplanes not equipped with the full IFR (instrument flight rules) instrument assembly.

8. Can assist in flight quality analysis and investigation of flight incidents for light aircraft and aircraft which are poorly equipped with modern flight and navigation equipment.

The appendices present a feedback from a pilot who helped to conduct the prototype trials.

The work does not describe how the system can help in the cases that are mentioned in Table 1.1. First of all, the developed method is more for standard flight cases than for the purpose of directly/solely reducing the number of incidents. Secondly, in order to apply the developed system to prevent accidents, it is mandatory to connect it to the aircraft's existing equipment and control organs. And in order to be prepared to prevent accidents, it is necessary to equip aeroplanes with auxiliary systems (for example, referred to "AC braking capability" section, or rocket brakes, which are used quite frequently in military aviation). However, all this requires a huge job of calculating each specific type of aircraft for the possibility of applying each particular braking device, forces, weights, costs, etc., which already looks like another subject for another doctoral thesis. As it was not planned to do so within the scope of this promotion work, no such analysis had been carried out.

In the course of further development, the device may be extended with additional line replaceable units (LRU) from other manufactures (GPS, Accelerometer, etc.), which may, first, increase the accuracy of the device and, secondly, allow it to become an autonomous device independent from AC INS and other systems. It is also possible to connect the device to AC equipment, which is likely to produce the best result. It is strongly recommended to increase the redundancy of the device: using certified microcontrollers and organizing a large number of processor systems as practiced in the avionics production process (at least two independent processors controlling each other).

Before testing and safety analysis is carried out, the device must be used as a separate device only providing additional information source, which does not affect the control organs of the aeroplane or any other equipment, therefore, the final decision will have to be taken by the crew of the aeroplane.

Artūrs Suharevs was born in 1990 in Riga. He obtained a Bachelor's degree in Aviation Transport from Riga Technical University in 2013 and a Master's degree in Aviation Transport in 2015. He has been a technitian at "PSAC Rigas Aeroklubs" Ltd. He is currently a certified B1/B2 technician of "Air Baltic Corporation" JSC and an instructor of "Air Baltic Training" Ltd. His main research interests are aviation safety and avionics.